

Two-Gluon Correlations in Heavy-Light Ion Collisions

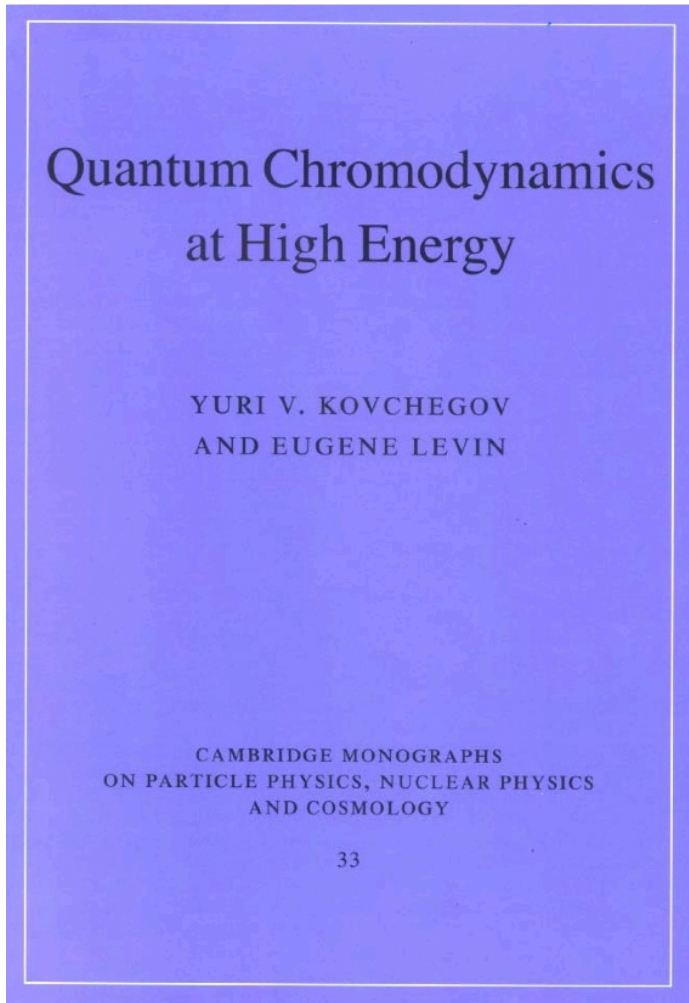
Yuri V. Kovchegov
The Ohio State University

work in collaboration with with Douglas Wertepny
arXiv:1212.1195 [hep-ph], arXiv:1310.6701 [hep-ph]

Outline

- Long-range rapidity correlations in hadronic and nuclear collisions: general discussion
- Two-gluon production in heavy-light ion collisions:
 - Geometric correlations
 - Long-range rapidity correlations
 - Even harmonics
 - Energy independence
 - Initial vs final state correlations
 - Perturbative HBT correlations
- k_T -factorization
- Conclusions

Introduction to saturation physics

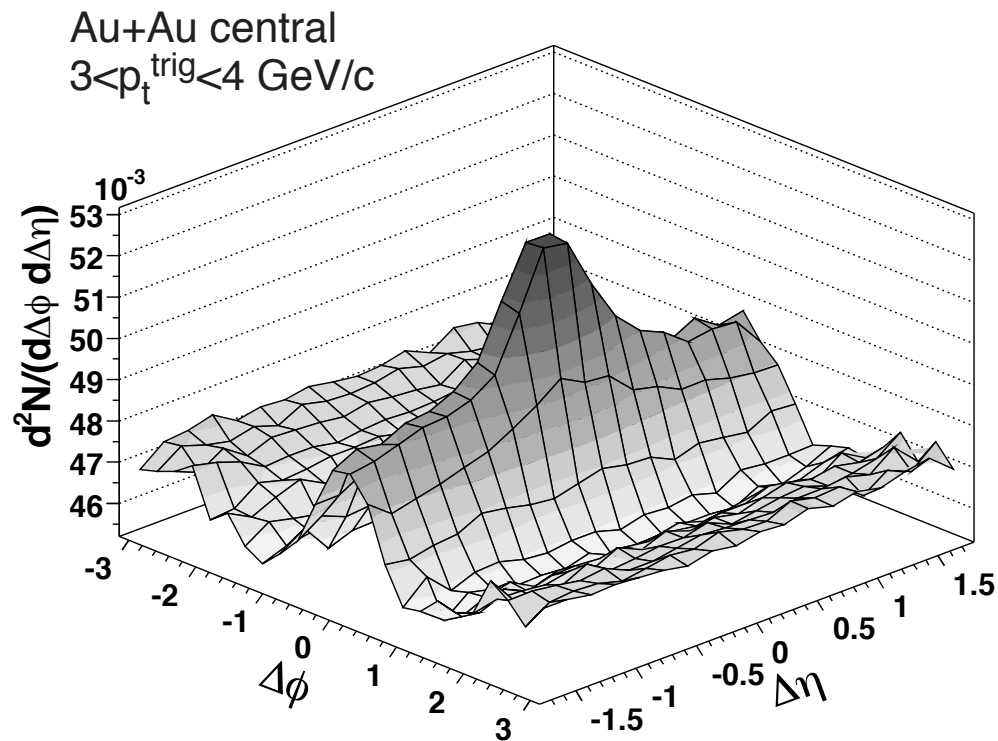


Published in September 2012
by Cambridge U Press

Long-range rapidity correlations

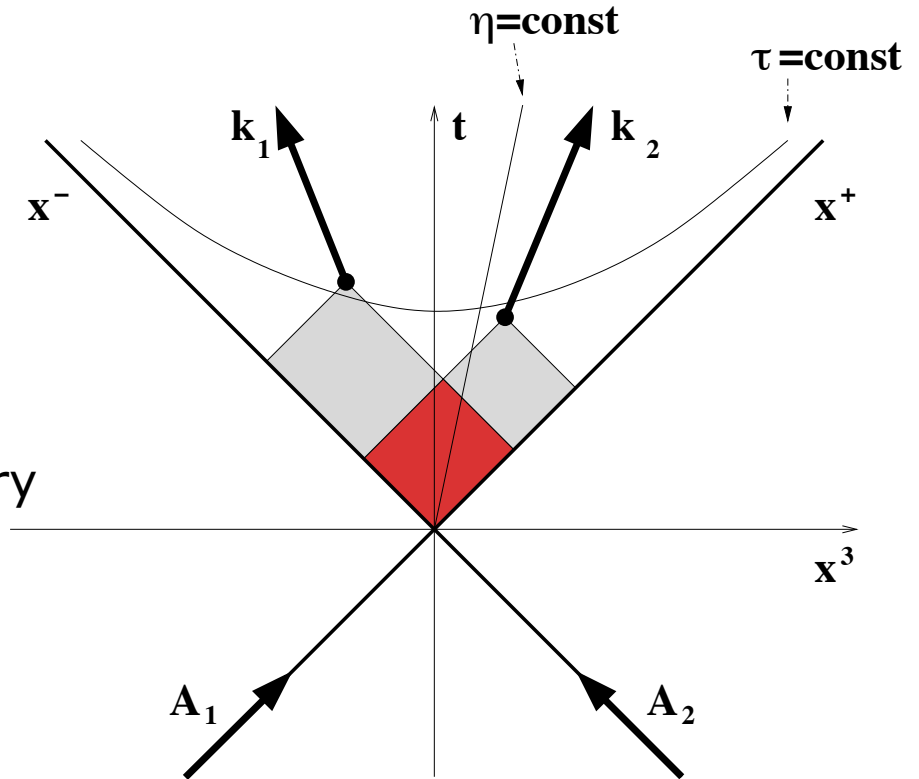
Ridge in heavy ion collisions

- Heavy ion collisions, along with high-multiplicity p+p and p+A collisions, are known to have long-range rapidity correlations, known as ‘the ridge’:



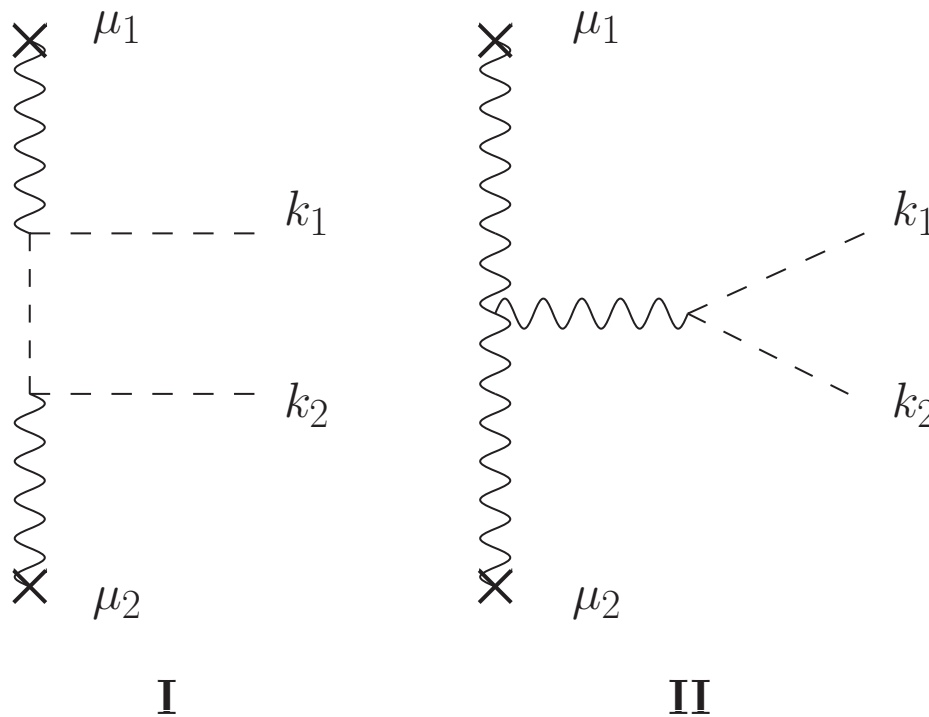
Origin of rapidity correlations

Causality demands that long-range rapidity correlations originate at very early times (cf. explanation of the CMB homogeneity in the Universe)



Gavin, McLerran, Moschelli '08;
Dumitru, Gelis, McLerran, Venugopalan '08.

Correlations in AdS shock wave collisions



$$C(k_1, k_2) \sim \cosh(4 \Delta y)$$

Correlations in AdS shock wave collisions

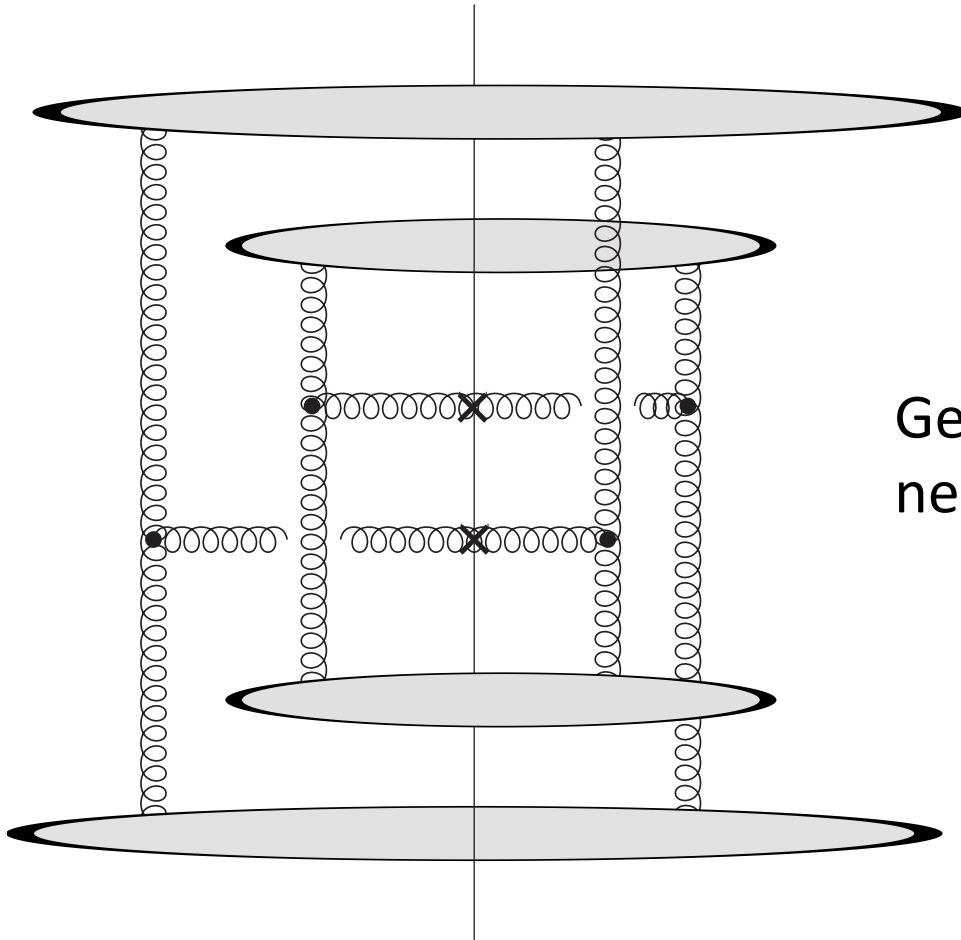
$$C(k_1, k_2) \sim \cosh(4 \Delta y)$$

- Correlations grow with rapidity interval???
- It is possible that higher-order corrections in shock wave strengths will modify this result, making it closer to real life.
- However, such corrections are important at later times, and are less likely to affect the long-range rapidity correlation...
- This could be another argument in favor of weakly-coupled dynamics in the early stages of heavy ion collisions.

Ridge in CGC

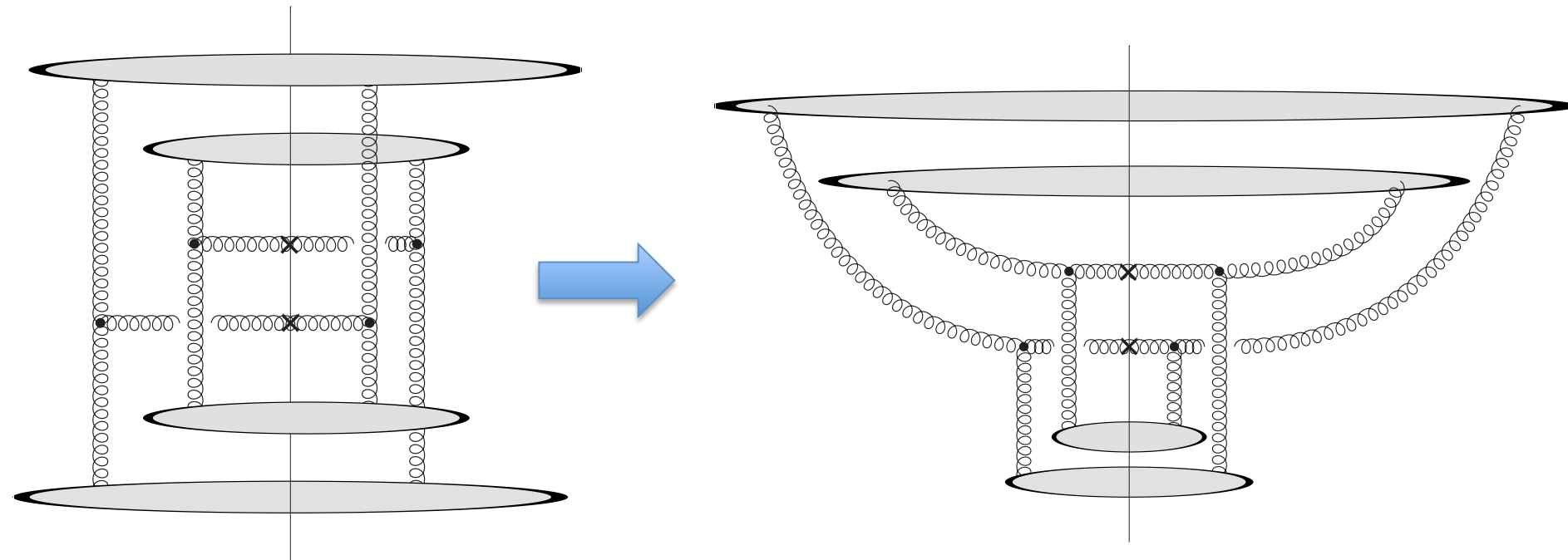
- There are two explanations of the ridge in CGC:
 - Long-range rapidity-independent fields are created at early times, with correlations generated soon after and with azimuthal collimation produced by radial hydro flow. (Gavin, McLerran, Moschelli '08)
 - Both long-range rapidity correlations and the azimuthal correlations are created in the collision due to a particular class of diagrams referred to as the “Glasma graphs”.

Glasma graphs



Generate back-to-back and near-side azimuthal correlations.

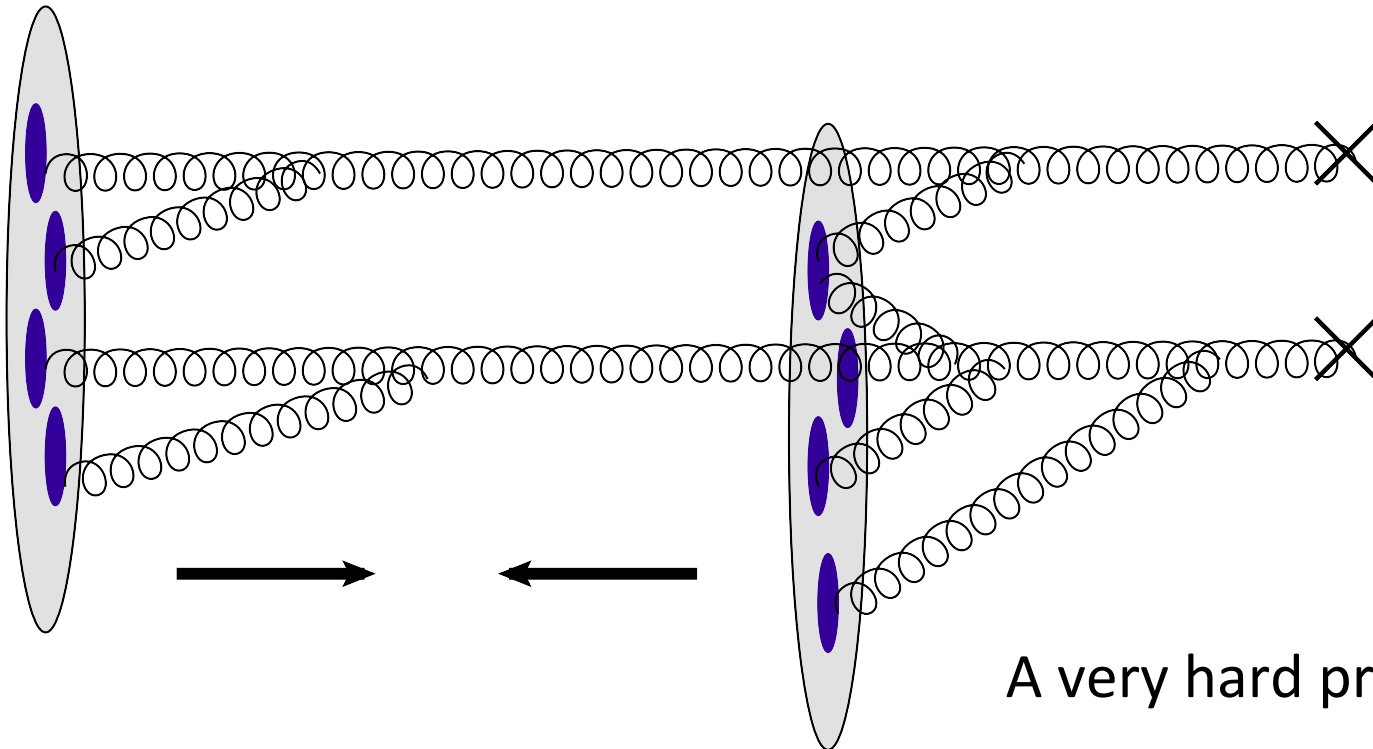
Glasma graphs in LC gauge



Glasma graphs are one of the many rescattering diagrams when two nucleons with a gluon each scatter on a nuclear target.

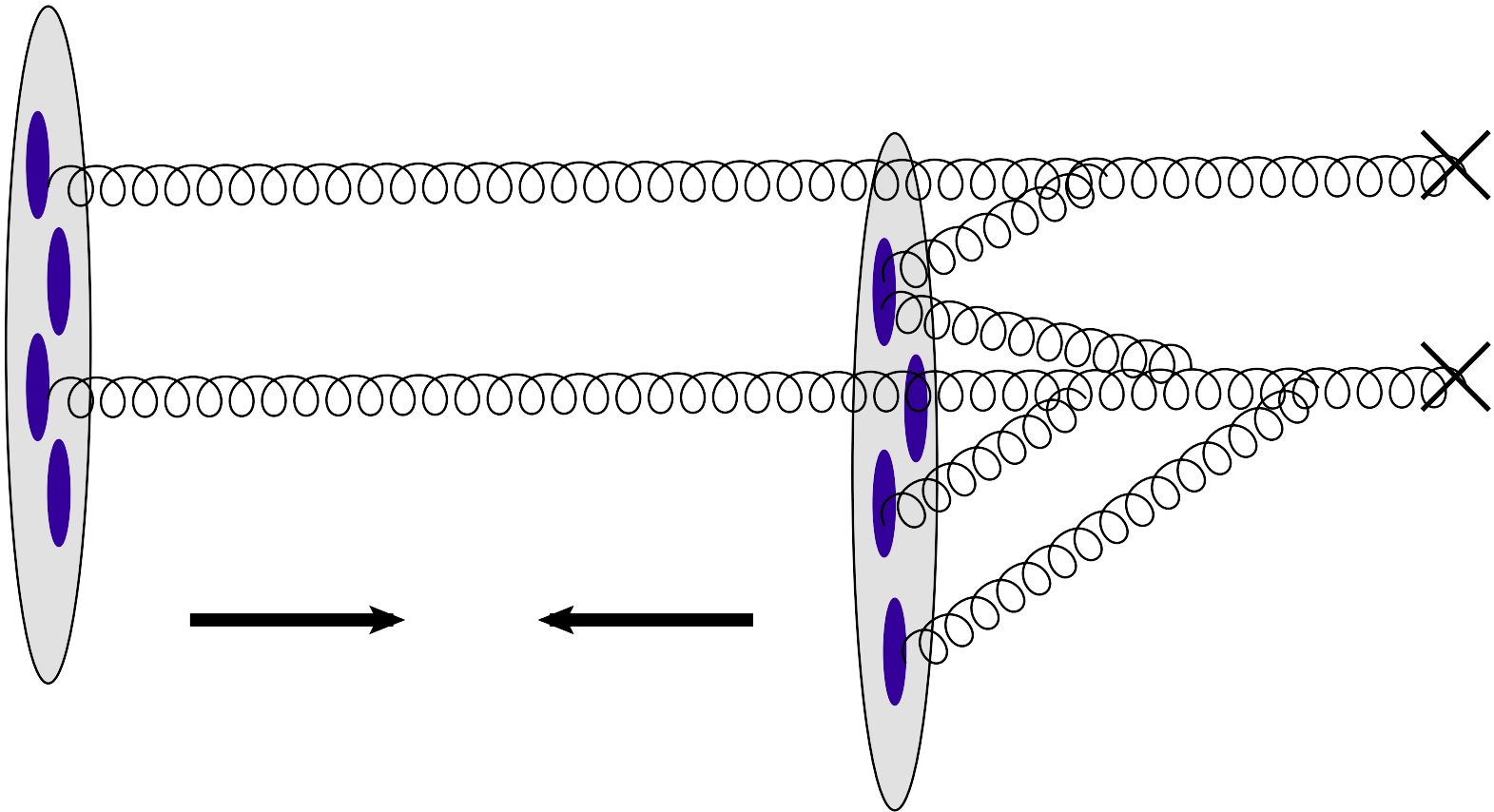
What to calculate?

- To systematically include Glasma graphs in the CGC formalism it would be great to solve the two-gluon inclusive production problem in the MV model, that is, including multiple rescatterings in both nuclei to all orders (the two produced gluons only talk to each other through sources):



A very hard problem!

Heavy-Light Ion Collisions



Little steps for the little feet: consider multiple rescatterings only in one of the two nuclei.

Double gluon production in heavy-light ion collisions

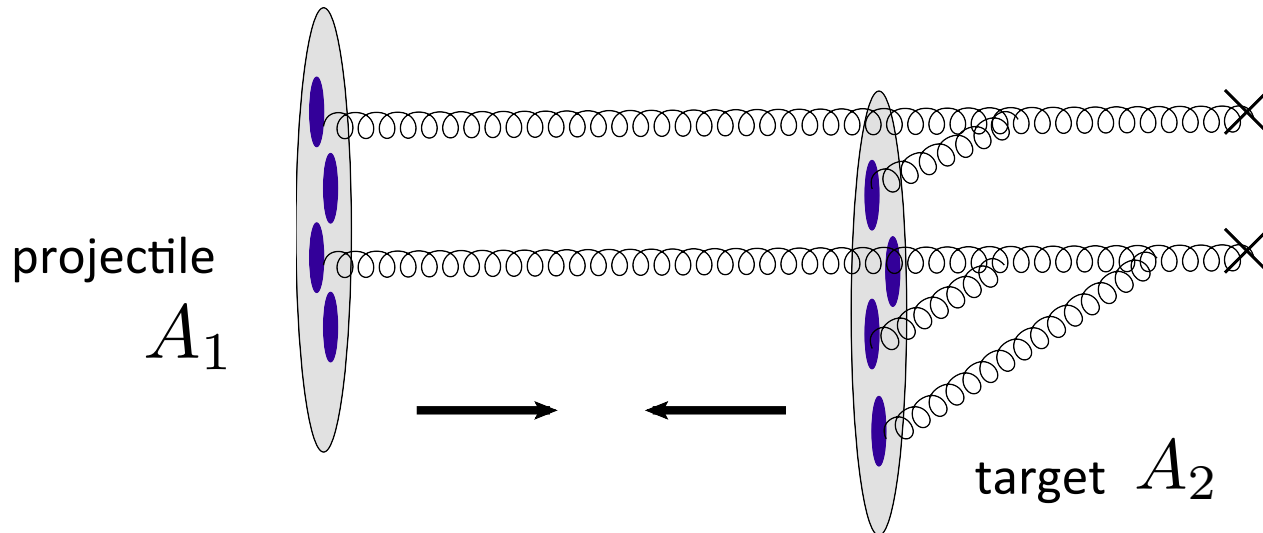
A. Setting up the problem: geometric correlations

Two-gluon production

- We want to calculate two gluon production in A_1+A_2 collisions with $1 \ll A_1 \ll A_2$ resumming all powers of

$$\alpha_s^2 A_2^{1/3} \sim 1 \quad \text{while} \quad \alpha_s^2 A_1^{1/3} \ll 1$$

(multiple rescatterings in the target nucleus)



- The gluons come from different nucleons in the projectile nucleus as $A_1 \gg 1$ and this is enhanced compared to emission from the same nucleon.

Applicability region

- The saturation scales of the two nuclei are very different:

$$\Lambda_{QCD} \ll Q_{s1} \ll Q_{s2}$$

- We are working above the saturation scale of the smaller nucleus:

$$k_T \gg Q_{s1}$$

- We thus sum all multiple rescatterings in the larger nucleus, $Q_{s2}/k_T \sim 1$, staying at the lowest non-trivial order in $Q_{s1}/k_T \ll 1$.
- Multiple interactions with the same nucleon in either nucleus are suppressed by $\Lambda_{QCD}/k_T \ll \ll 1$.

Production cross-section

- The single- and double-inclusive cross sections can be written as

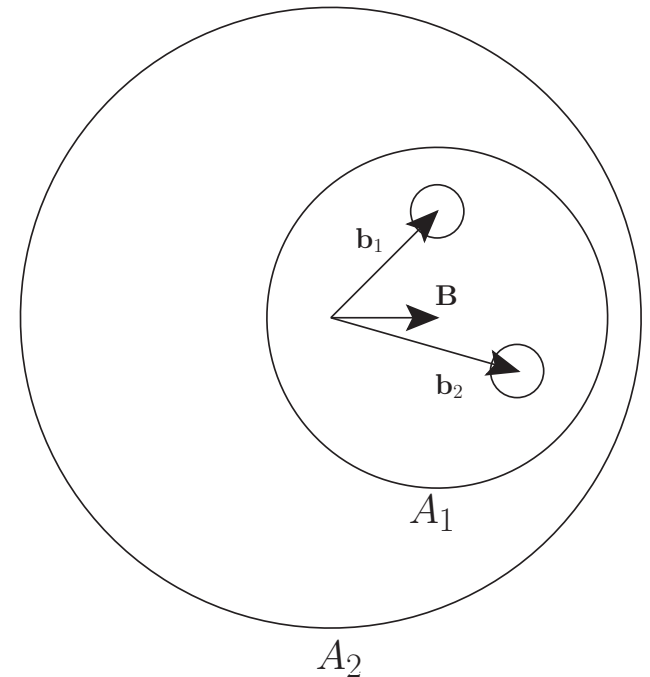
$$\frac{d\sigma}{d^2k dy} = \int d^2B d^2b |\Psi_I(\mathbf{B} - \mathbf{b})|^2 \left\langle \frac{d\sigma^{pA_2}}{d^2k dy d^2b} \right\rangle$$

$$\frac{d\sigma}{d^2k_1 dy_1 d^2k_2 dy_2} = \int d^2B d^2b_1 d^2b_2 |\Psi_{II}(\mathbf{B} - \mathbf{b}_1, \mathbf{B} - \mathbf{b}_2)|^2 \left\langle \frac{d\sigma^{pA_2}}{d^2k_1 dy_1 d^2b_1} \frac{d\sigma^{pA_2}}{d^2k_2 dy_2 d^2b_2} \right\rangle$$

- Assume a large nucleus with uncorrelated nucleons (MV/Glauber model). Then the single- and double-nucleon wave functions are (with T_1 the nuclear profile function)

$$|\Psi_I(\mathbf{b})|^2 = T_1(\mathbf{b})$$

$$|\Psi_{II}(\mathbf{b}_1, \mathbf{b}_2)|^2 = T_1(\mathbf{b}_1) T_1(\mathbf{b}_2)$$



Geometric Correlations

- Assume uncorrelated interaction with the target:

$$\left\langle \frac{d\sigma^{pA_2}}{d^2k_1 dy_1 d^2b_1} \frac{d\sigma^{pA_2}}{d^2k_2 dy_2 d^2b_2} \right\rangle \approx \left\langle \frac{d\sigma^{pA_2}}{d^2k_1 dy_1 d^2b_1} \right\rangle \left\langle \frac{d\sigma^{pA_2}}{d^2k_2 dy_2 d^2b_2} \right\rangle$$

- For cross sections we have

$$\frac{d\sigma}{d^2k dy} = \int d^2B d^2b T_1(\mathbf{B} - \mathbf{b}) \left\langle \frac{d\sigma^{pA_2}}{d^2k dy d^2b} \right\rangle$$

$$\frac{d\sigma}{d^2k_1 dy_1 d^2k_2 dy_2} = \int d^2B d^2b_1 d^2b_2 T_1(\mathbf{B} - \mathbf{b}_1) T_1(\mathbf{B} - \mathbf{b}_2) \left\langle \frac{d\sigma^{pA_2}}{d^2k_1 dy_1 d^2b_1} \right\rangle \left\langle \frac{d\sigma^{pA_2}}{d^2k_2 dy_2 d^2b_2} \right\rangle$$

- Clearly

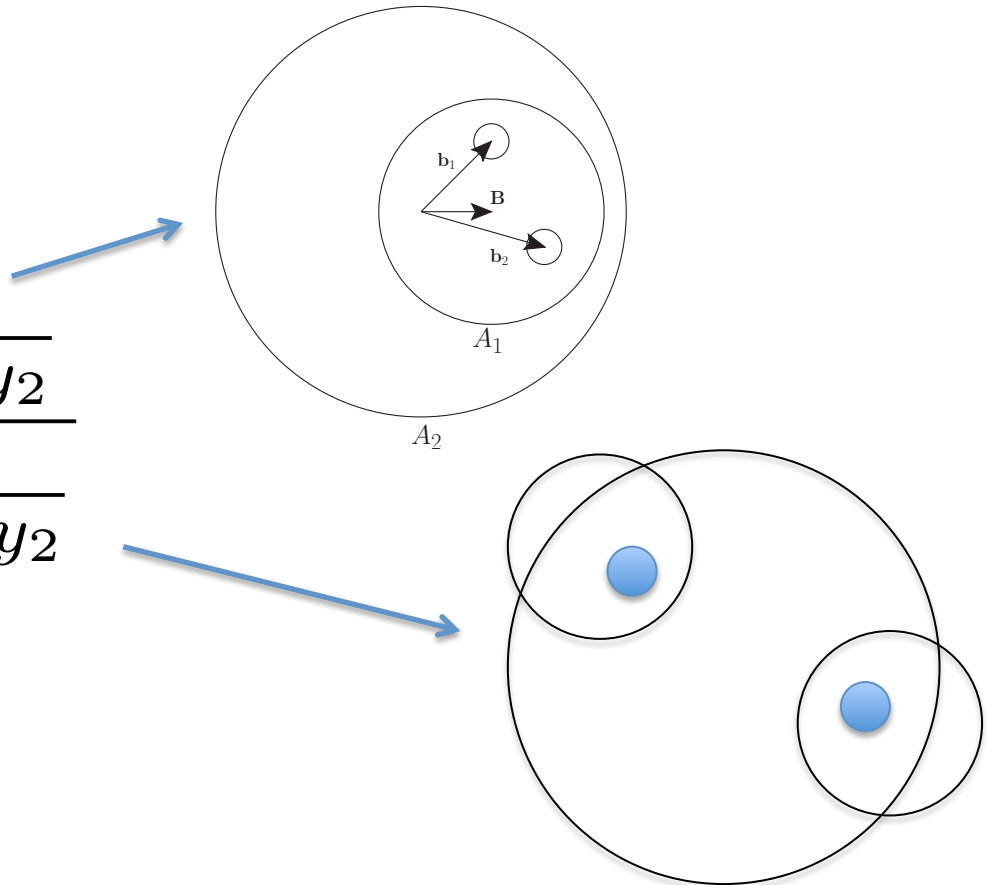
$$\frac{d\sigma}{d^2k_1 dy_1 d^2k_2 dy_2} \approx \frac{d\sigma}{d^2k_1 dy_1} \frac{d\sigma}{d^2k_2 dy_2}$$

- Correlations due to the integration over the impact parameter B
-> **Geometric correlations!**

Geometric correlations: physical meaning

- In the same event the two nucleons are always within the smaller nucleus diameter from each other (in transverse nucleus).

$$C \propto \frac{\frac{d\sigma}{d^2k_1 dy_1 d^2k_2 dy_2}}{\frac{d\sigma}{d^2k_1 dy_1} \frac{d\sigma}{d^2k_2 dy_2}}$$



Geometric correlations at fixed B

- are zero as

$$\frac{d\sigma}{d^2 k_1 dy_1 d^2 k_2 dy_2 d^2 B} = \frac{d\sigma}{d^2 k_1 dy_1 d^2 B} \frac{d\sigma}{d^2 k_2 dy_2 d^2 B}$$

which is clear from

$$\frac{d\sigma}{d^2 k dy} = \int d^2 B d^2 b T_1(\mathbf{B} - \mathbf{b}) \left\langle \frac{d\sigma^{pA_2}}{d^2 k dy d^2 b} \right\rangle$$

$$\frac{d\sigma}{d^2 k_1 dy_1 d^2 k_2 dy_2} = \int d^2 B d^2 b_1 d^2 b_2 T_1(\mathbf{B} - \mathbf{b}_1) T_1(\mathbf{B} - \mathbf{b}_2) \left\langle \frac{d\sigma^{pA_2}}{d^2 k_1 dy_1 d^2 b_1} \right\rangle \left\langle \frac{d\sigma^{pA_2}}{d^2 k_2 dy_2 d^2 b_2} \right\rangle$$

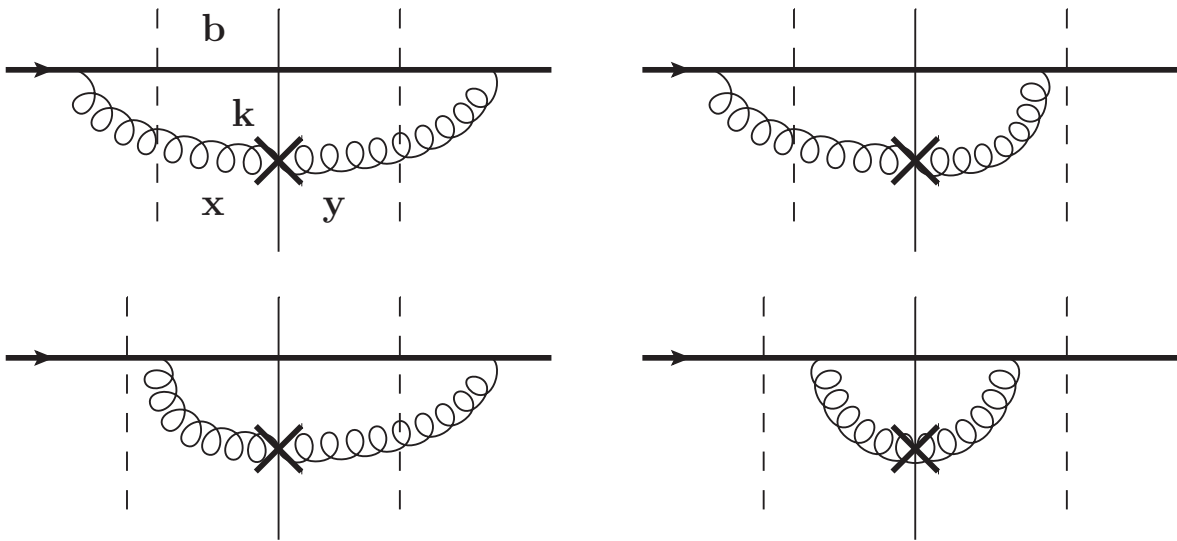
- Note that direction of B has to be fixed (to remove the geometric correlations), in other words the *vector* B should be fixed with respect to *vectors* k_1 and k_2 . Maybe hard to do, but perhaps possible.

B. Two-gluon production

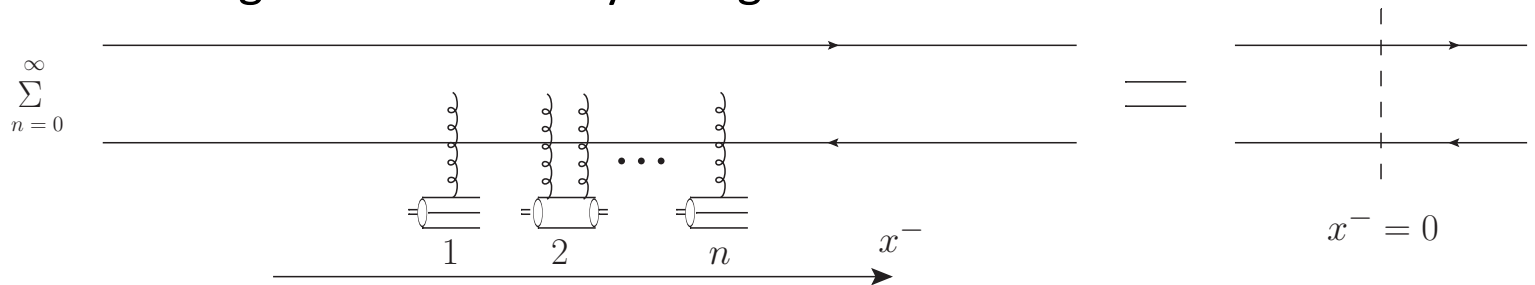
(i) Single gluon production in pA

Single gluon production in pA

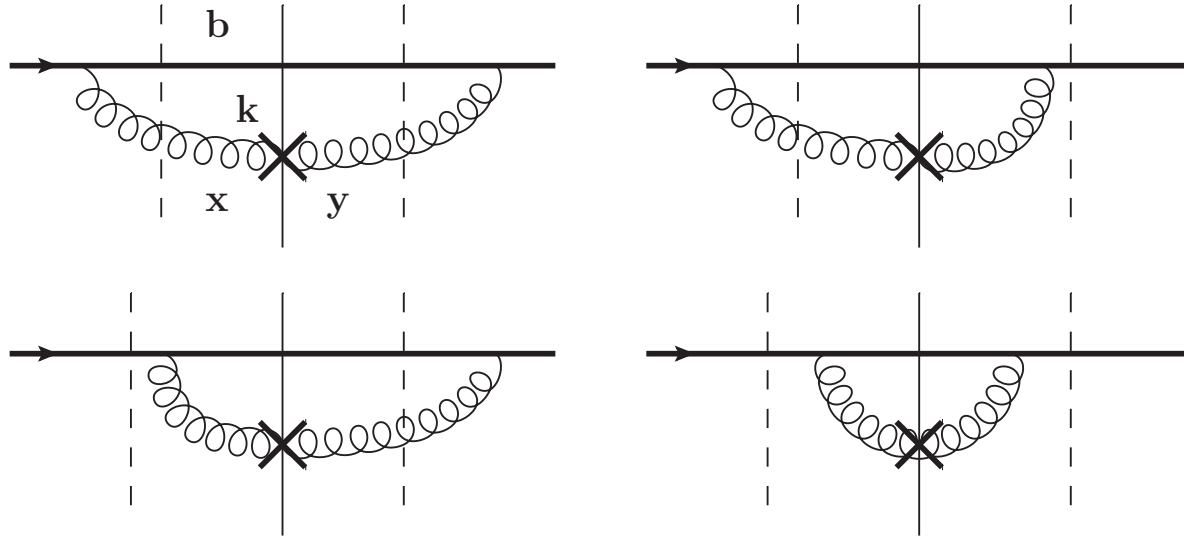
Model the proton by a single quark (can be easily improved upon).
 The diagrams are shown below (Yu.K., A. Mueller '97):



Multiple rescatterings are denoted by a single dashed line:



Single gluon production in pA



The gluon production cross section can be readily written as (U = Wilson line in **adjoint** representation, represents gluon interactions with the target)

$$\left\langle \frac{d\sigma^{pA_2}}{d^2k dy d^2b} \right\rangle = \frac{\alpha_s C_F}{4\pi^4} \int d^2x d^2y e^{-i\mathbf{k}\cdot(\mathbf{x}-\mathbf{y})} \frac{\mathbf{x}-\mathbf{b}}{|\mathbf{x}-\mathbf{b}|^2} \cdot \frac{\mathbf{y}-\mathbf{b}}{|\mathbf{y}-\mathbf{b}|^2} \\ \times \left\langle \frac{1}{N_c^2 - 1} \text{Tr}[U_{\mathbf{x}} U_{\mathbf{y}}^\dagger] - \frac{1}{N_c^2 - 1} \text{Tr}[U_{\mathbf{x}} U_{\mathbf{b}}^\dagger] - \frac{1}{N_c^2 - 1} \text{Tr}[U_{\mathbf{b}} U_{\mathbf{y}}^\dagger] + 1 \right\rangle$$

Forward dipole amplitude

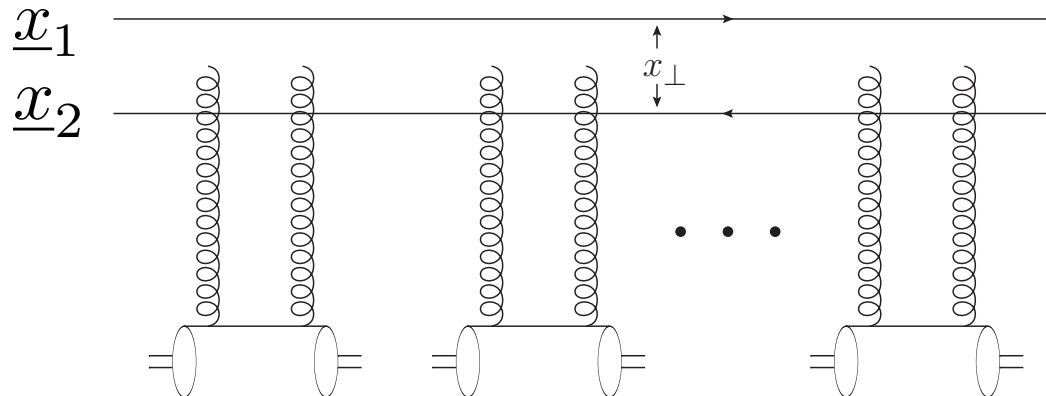
- The eikonal quark propagator is given by the Wilson line

$$V(\underline{x}) = \text{P exp} \left[i g \int_{-\infty}^{\infty} dx^+ A^-(x^+, x^- = 0, \underline{x}) \right]$$

The
eikonal

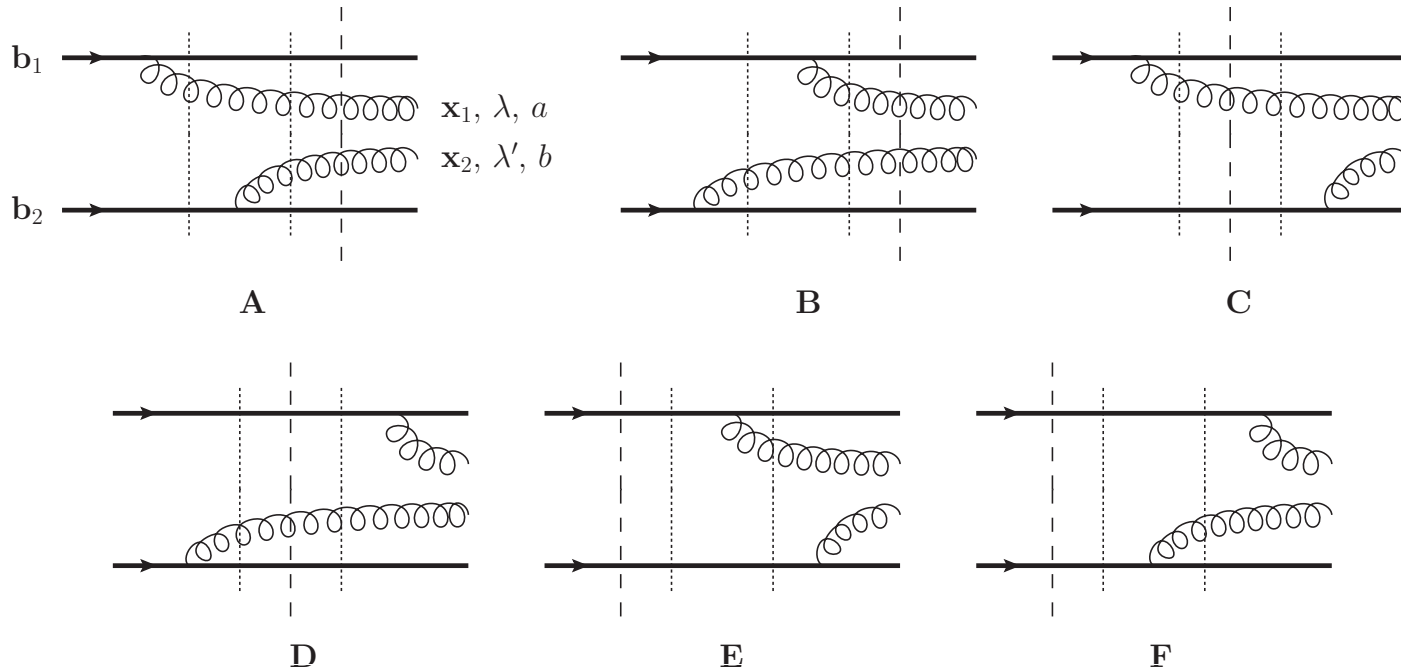
quark propagator is given by the Wilson line

$$N(\underline{x}_1, \underline{x}_2) = \frac{1}{N} \text{tr} V(\underline{x}_1) V(\underline{x}_2)$$



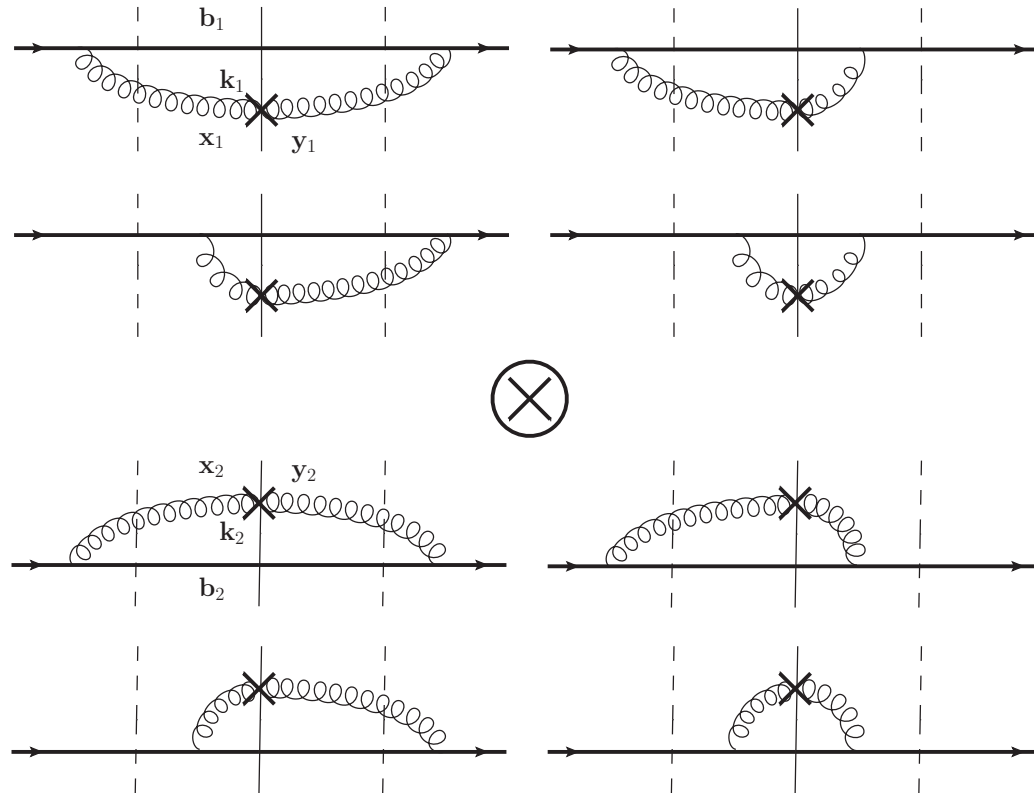
(ii) Two-gluon production
in heavy-light ion collisions

The process



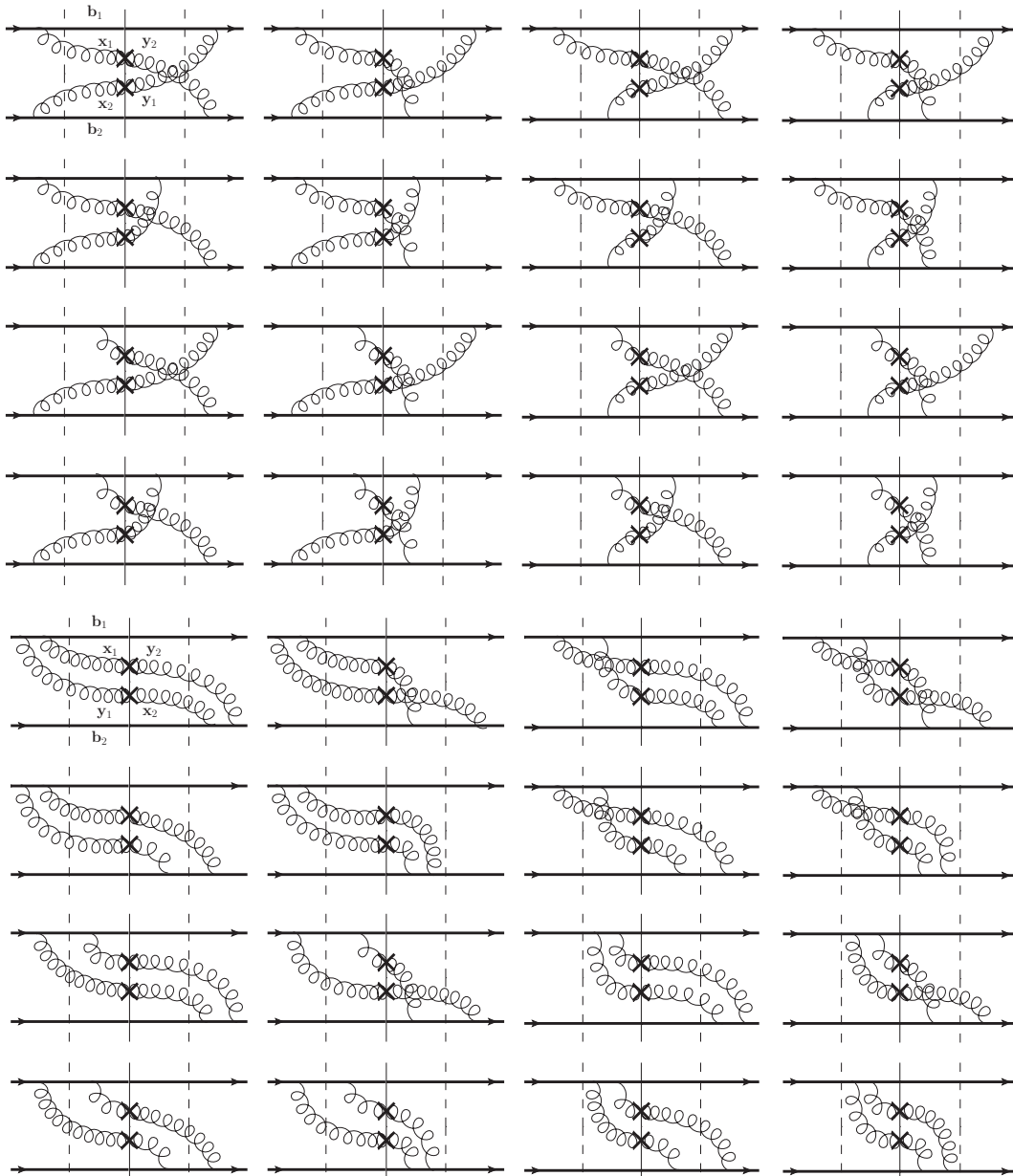
Solid horizontal lines = quarks in the incoming nucleons.
 Dashed vertical line = interaction with the target.
 Dotted vertical lines = energy denominators (ignore).

Amplitude squared



This contribution to two-gluon production looks like one-gluon production squared, with the target averaging applied to both.

Amplitude squared

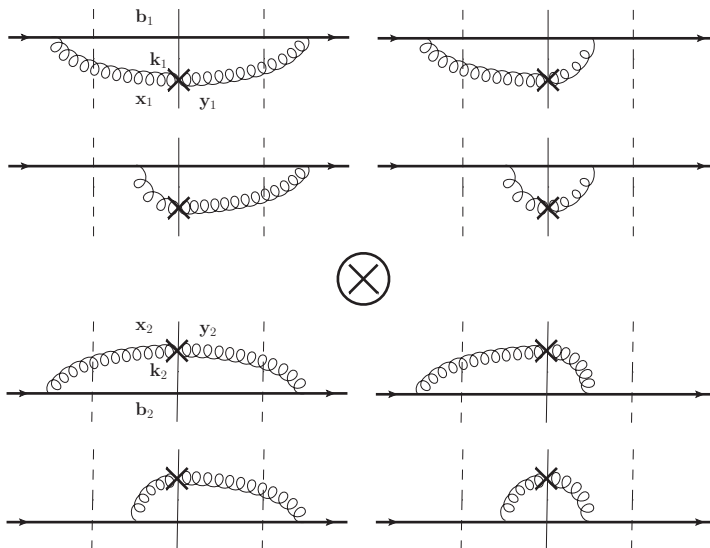


These contributions to two-gluon production contain cross-talk between the emissions from different nucleons.

Two-gluon production cross section

- “Squaring” the single gluon production cross section yields

$$\begin{aligned} \frac{d\sigma}{d^2k_1 dy_1 d^2k_2 dy_2} &= \frac{\alpha_s^2 C_F^2}{16 \pi^8} \int d^2B d^2b_1 d^2b_2 T_1(\mathbf{B} - \mathbf{b}_1) T_1(\mathbf{B} - \mathbf{b}_2) d^2x_1 d^2y_1 d^2x_2 d^2y_2 e^{-i \mathbf{k}_1 \cdot (\mathbf{x}_1 - \mathbf{y}_1) - i \mathbf{k}_2 \cdot (\mathbf{x}_2 - \mathbf{y}_2)} \\ &\times \frac{\mathbf{x}_1 - \mathbf{b}_1}{|\mathbf{x}_1 - \mathbf{b}_1|^2} \cdot \frac{\mathbf{y}_1 - \mathbf{b}_1}{|\mathbf{y}_1 - \mathbf{b}_1|^2} \frac{\mathbf{x}_2 - \mathbf{b}_2}{|\mathbf{x}_2 - \mathbf{b}_2|^2} \cdot \frac{\mathbf{y}_2 - \mathbf{b}_2}{|\mathbf{y}_2 - \mathbf{b}_2|^2} \\ &\times \left\langle \left(\frac{1}{N_c^2 - 1} \text{Tr}[U_{\mathbf{x}_1} U_{\mathbf{y}_1}^\dagger] - \frac{1}{N_c^2 - 1} \text{Tr}[U_{\mathbf{x}_1} U_{\mathbf{b}_1}^\dagger] - \frac{1}{N_c^2 - 1} \text{Tr}[U_{\mathbf{b}_1} U_{\mathbf{y}_1}^\dagger] + 1 \right) \right. \\ &\times \left. \left(\frac{1}{N_c^2 - 1} \text{Tr}[U_{\mathbf{x}_2} U_{\mathbf{y}_2}^\dagger] - \frac{1}{N_c^2 - 1} \text{Tr}[U_{\mathbf{x}_2} U_{\mathbf{b}_2}^\dagger] - \frac{1}{N_c^2 - 1} \text{Tr}[U_{\mathbf{b}_2} U_{\mathbf{y}_2}^\dagger] + 1 \right) \right\rangle \end{aligned}$$

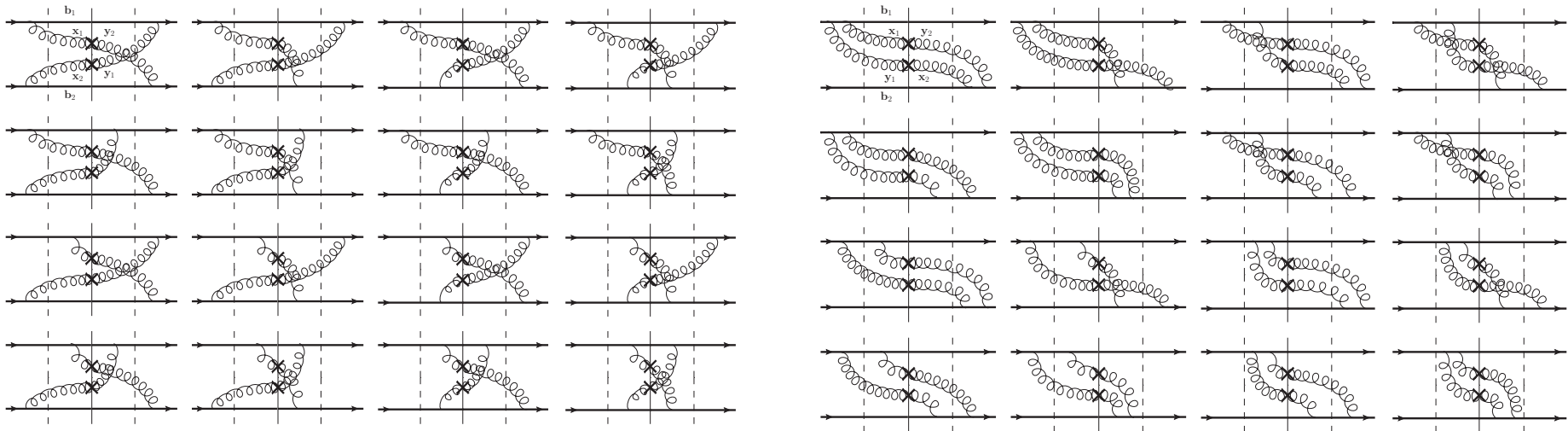


(cf. Kovner & Lublinsky, '12)

Two-gluon production cross section

- The “crossed” diagrams give

$$\begin{aligned} \frac{d\sigma_{crossed}}{d^2k_1 dy_1 d^2k_2 dy_2} &= \frac{1}{[2(2\pi)^3]^2} \int d^2B d^2b_1 d^2b_2 T_1(\mathbf{B} - \mathbf{b}_1) T_1(\mathbf{B} - \mathbf{b}_2) d^2x_1 d^2y_1 d^2x_2 d^2y_2 \\ &\times \left[e^{-i\mathbf{k}_1 \cdot (\mathbf{x}_1 - \mathbf{y}_2) - i\mathbf{k}_2 \cdot (\mathbf{x}_2 - \mathbf{y}_1)} + e^{-i\mathbf{k}_1 \cdot (\mathbf{x}_1 - \mathbf{y}_2) + i\mathbf{k}_2 \cdot (\mathbf{x}_2 - \mathbf{y}_1)} \right] \\ &\times \frac{16\alpha_s^2}{\pi^2} \frac{C_F}{2N_c} \frac{\mathbf{x}_1 - \mathbf{b}_1}{|\mathbf{x}_1 - \mathbf{b}_1|^2} \cdot \frac{\mathbf{y}_2 - \mathbf{b}_2}{|\mathbf{y}_2 - \mathbf{b}_2|^2} \frac{\mathbf{x}_2 - \mathbf{b}_2}{|\mathbf{x}_2 - \mathbf{b}_2|^2} \cdot \frac{\mathbf{y}_1 - \mathbf{b}_1}{|\mathbf{y}_1 - \mathbf{b}_1|^2} \\ &\times \left[Q(\mathbf{x}_1, \mathbf{y}_1, \mathbf{x}_2, \mathbf{y}_2) - Q(\mathbf{x}_1, \mathbf{y}_1, \mathbf{x}_2, \mathbf{b}_2) - Q(\mathbf{x}_1, \mathbf{y}_1, \mathbf{b}_2, \mathbf{y}_2) + S_G(\mathbf{x}_1, \mathbf{y}_1) - Q(\mathbf{x}_1, \mathbf{b}_1, \mathbf{x}_2, \mathbf{y}_2) \right. \\ &+ Q(\mathbf{x}_1, \mathbf{b}_1, \mathbf{x}_2, \mathbf{b}_2) + Q(\mathbf{x}_1, \mathbf{b}_1, \mathbf{b}_2, \mathbf{y}_2) - S_G(\mathbf{x}_1, \mathbf{b}_1) - Q(\mathbf{b}_1, \mathbf{y}_1, \mathbf{x}_2, \mathbf{y}_2) + Q(\mathbf{b}_1, \mathbf{y}_1, \mathbf{x}_2, \mathbf{b}_2) \\ &\left. + Q(\mathbf{b}_1, \mathbf{y}_1, \mathbf{b}_2, \mathbf{y}_2) - S_G(\mathbf{b}_1, \mathbf{y}_1) + S_G(\mathbf{x}_2, \mathbf{y}_2) - S_G(\mathbf{x}_2, \mathbf{b}_2) - S_G(\mathbf{b}_2, \mathbf{y}_2) + 1 \right] \end{aligned}$$



Two-gluon production cross section

- The “crossed” diagrams give

$$\begin{aligned}
 \frac{d\sigma_{crossed}}{d^2k_1 dy_1 d^2k_2 dy_2} &= \frac{1}{[2(2\pi)^3]^2} \int d^2B d^2b_1 d^2b_2 T_1(\mathbf{B} - \mathbf{b}_1) T_1(\mathbf{B} - \mathbf{b}_2) d^2x_1 d^2y_1 d^2x_2 d^2y_2 \\
 &\times \left[e^{-i\mathbf{k}_1 \cdot (\mathbf{x}_1 - \mathbf{y}_2) - i\mathbf{k}_2 \cdot (\mathbf{x}_2 - \mathbf{y}_1)} + e^{-i\mathbf{k}_1 \cdot (\mathbf{x}_1 - \mathbf{y}_2) + i\mathbf{k}_2 \cdot (\mathbf{x}_2 - \mathbf{y}_1)} \right] \\
 &\times \frac{16\alpha_s^2}{\pi^2} \frac{C_F}{2N_c} \frac{\mathbf{x}_1 - \mathbf{b}_1}{|\mathbf{x}_1 - \mathbf{b}_1|^2} \cdot \frac{\mathbf{y}_2 - \mathbf{b}_2}{|\mathbf{y}_2 - \mathbf{b}_2|^2} \frac{\mathbf{x}_2 - \mathbf{b}_2}{|\mathbf{x}_2 - \mathbf{b}_2|^2} \cdot \frac{\mathbf{y}_1 - \mathbf{b}_1}{|\mathbf{y}_1 - \mathbf{b}_1|^2} \\
 &\times \left[Q(\mathbf{x}_1, \mathbf{y}_1, \mathbf{x}_2, \mathbf{y}_2) - Q(\mathbf{x}_1, \mathbf{y}_1, \mathbf{x}_2, \mathbf{b}_2) - Q(\mathbf{x}_1, \mathbf{y}_1, \mathbf{b}_2, \mathbf{y}_2) + S_G(\mathbf{x}_1, \mathbf{y}_1) - Q(\mathbf{x}_1, \mathbf{b}_1, \mathbf{x}_2, \mathbf{y}_2) \right. \\
 &+ Q(\mathbf{x}_1, \mathbf{b}_1, \mathbf{x}_2, \mathbf{b}_2) + Q(\mathbf{x}_1, \mathbf{b}_1, \mathbf{b}_2, \mathbf{y}_2) - S_G(\mathbf{x}_1, \mathbf{b}_1) - Q(\mathbf{b}_1, \mathbf{y}_1, \mathbf{x}_2, \mathbf{y}_2) + Q(\mathbf{b}_1, \mathbf{y}_1, \mathbf{x}_2, \mathbf{b}_2) \\
 &\left. + Q(\mathbf{b}_1, \mathbf{y}_1, \mathbf{b}_2, \mathbf{y}_2) - S_G(\mathbf{b}_1, \mathbf{y}_1) + S_G(\mathbf{x}_2, \mathbf{y}_2) - S_G(\mathbf{x}_2, \mathbf{b}_2) - S_G(\mathbf{b}_2, \mathbf{y}_2) + 1 \right]
 \end{aligned}$$

- We introduced the adjoint color-dipole and color quadrupole amplitudes:

$$S_G(\mathbf{x}_1, \mathbf{x}_2, y) \equiv \frac{1}{N_c^2 - 1} \langle \text{Tr}[U_{\mathbf{x}_1} U_{\mathbf{x}_2}^\dagger] \rangle$$

$$Q(\mathbf{x}_1, \mathbf{x}_2, \mathbf{x}_3, \mathbf{x}_4) \equiv \frac{1}{N_c^2 - 1} \langle \text{Tr}[U_{\mathbf{x}_1} U_{\mathbf{x}_2}^\dagger U_{\mathbf{x}_3} U_{\mathbf{x}_4}^\dagger] \rangle$$

Two-gluon production: properties

$$\begin{aligned}
 \frac{d\sigma}{d^2k_1 dy_1 d^2k_2 dy_2} &= \frac{\alpha_s^2 C_F^2}{16 \pi^8} \int d^2B d^2b_1 d^2b_2 T_1(\mathbf{B} - \mathbf{b}_1) T_1(\mathbf{B} - \mathbf{b}_2) d^2x_1 d^2y_1 d^2x_2 d^2y_2 e^{-i \mathbf{k}_1 \cdot (\mathbf{x}_1 - \mathbf{y}_1) - i \mathbf{k}_2 \cdot (\mathbf{x}_2 - \mathbf{y}_2)} \\
 &\times \frac{\mathbf{x}_1 - \mathbf{b}_1}{|\mathbf{x}_1 - \mathbf{b}_1|^2} \cdot \frac{\mathbf{y}_1 - \mathbf{b}_1}{|\mathbf{y}_1 - \mathbf{b}_1|^2} \frac{\mathbf{x}_2 - \mathbf{b}_2}{|\mathbf{x}_2 - \mathbf{b}_2|^2} \cdot \frac{\mathbf{y}_2 - \mathbf{b}_2}{|\mathbf{y}_2 - \mathbf{b}_2|^2} \\
 &\times \left\langle \left(\frac{1}{N_c^2 - 1} \text{Tr}[U_{\mathbf{x}_1} U_{\mathbf{y}_1}^\dagger] - \frac{1}{N_c^2 - 1} \text{Tr}[U_{\mathbf{x}_1} U_{\mathbf{b}_1}^\dagger] - \frac{1}{N_c^2 - 1} \text{Tr}[U_{\mathbf{b}_1} U_{\mathbf{y}_1}^\dagger] + 1 \right) \right. \\
 &\times \left. \left(\frac{1}{N_c^2 - 1} \text{Tr}[U_{\mathbf{x}_2} U_{\mathbf{y}_2}^\dagger] - \frac{1}{N_c^2 - 1} \text{Tr}[U_{\mathbf{x}_2} U_{\mathbf{b}_2}^\dagger] - \frac{1}{N_c^2 - 1} \text{Tr}[U_{\mathbf{b}_2} U_{\mathbf{y}_2}^\dagger] + 1 \right) \right\rangle
 \end{aligned}$$

- Note that if the interaction with the target factorizes,

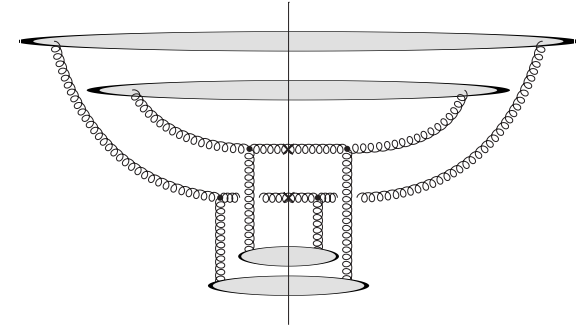
$$\left\langle \text{Tr}[U_{\mathbf{x}_1} U_{\mathbf{y}_1}^\dagger] \text{Tr}[U_{\mathbf{x}_2} U_{\mathbf{y}_2}^\dagger] \right\rangle \Big|_{\text{large-}N_c, \text{large-}A_2} \approx \left\langle \text{Tr}[U_{\mathbf{x}_1} U_{\mathbf{y}_1}^\dagger] \right\rangle \left\langle \text{Tr}[U_{\mathbf{x}_2} U_{\mathbf{y}_2}^\dagger] \right\rangle$$

we still have **the geometric correlations**.

- The geometric correlations lead to non-zero cumulants! (Like everything that depends on geometry.)

Two-gluon production: properties

$$\begin{aligned} \frac{d\sigma}{d^2k_1 dy_1 d^2k_2 dy_2} &= \frac{\alpha_s^2 C_F^2}{16 \pi^8} \int d^2B d^2b_1 d^2b_2 T_1(\mathbf{B} - \mathbf{b}_1) T_1(\mathbf{B} - \mathbf{b}_2) d^2x_1 d^2y_1 d^2x_2 d^2y_2 e^{-i \mathbf{k}_1 \cdot (\mathbf{x}_1 - \mathbf{y}_1) - i \mathbf{k}_2 \cdot (\mathbf{x}_2 - \mathbf{y}_2)} \\ &\times \frac{\mathbf{x}_1 - \mathbf{b}_1}{|\mathbf{x}_1 - \mathbf{b}_1|^2} \cdot \frac{\mathbf{y}_1 - \mathbf{b}_1}{|\mathbf{y}_1 - \mathbf{b}_1|^2} \frac{\mathbf{x}_2 - \mathbf{b}_2}{|\mathbf{x}_2 - \mathbf{b}_2|^2} \cdot \frac{\mathbf{y}_2 - \mathbf{b}_2}{|\mathbf{y}_2 - \mathbf{b}_2|^2} \\ &\times \left\langle \left(\frac{1}{N_c^2 - 1} \text{Tr}[U_{\mathbf{x}_1} U_{\mathbf{y}_1}^\dagger] - \frac{1}{N_c^2 - 1} \text{Tr}[U_{\mathbf{x}_1} U_{\mathbf{b}_1}^\dagger] - \frac{1}{N_c^2 - 1} \text{Tr}[U_{\mathbf{b}_1} U_{\mathbf{y}_1}^\dagger] + 1 \right) \right. \\ &\times \left. \left(\frac{1}{N_c^2 - 1} \text{Tr}[U_{\mathbf{x}_2} U_{\mathbf{y}_2}^\dagger] - \frac{1}{N_c^2 - 1} \text{Tr}[U_{\mathbf{x}_2} U_{\mathbf{b}_2}^\dagger] - \frac{1}{N_c^2 - 1} \text{Tr}[U_{\mathbf{b}_2} U_{\mathbf{y}_2}^\dagger] + 1 \right) \right\rangle \end{aligned}$$



- If we expand the interaction with the target to the lowest non-trivial order, one reproduced the contribution of the 'glasma' graphs:

$$\left. \frac{d\sigma_{corr}}{d^2k_1 dy_1 d^2k_2 dy_2} \right|_{LO} = \frac{\alpha_s^2}{4 \pi^4} \int d^2B d^2b [T_1(\mathbf{B} - \mathbf{b})]^2 \frac{Q_{s0}^4(\mathbf{b})}{\mathbf{k}_1^2 \mathbf{k}_2^2} \int_{\Lambda} \frac{d^2l}{(l^2)^2} \left[\frac{1}{(\mathbf{k}_1 - \mathbf{l})^2 (\mathbf{k}_2 + \mathbf{l})^2} + \frac{1}{(\mathbf{k}_1 - \mathbf{l})^2 (\mathbf{k}_2 - \mathbf{l})^2} \right]$$

away-side correlations

$$\sim \frac{1}{(\mathbf{k}_1 + \mathbf{k}_2)^2}$$

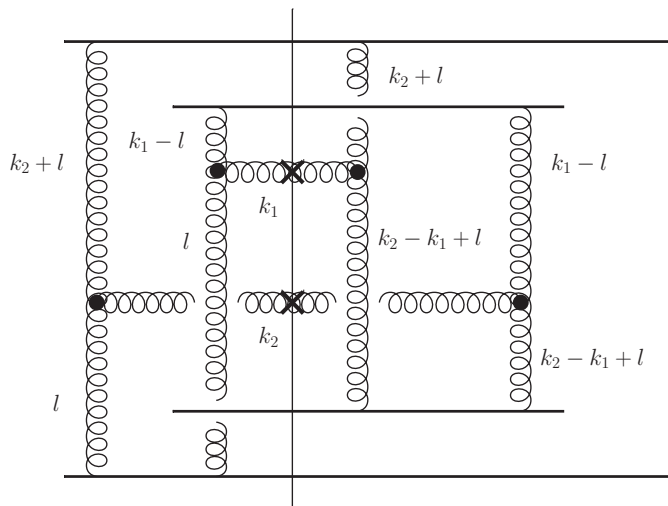
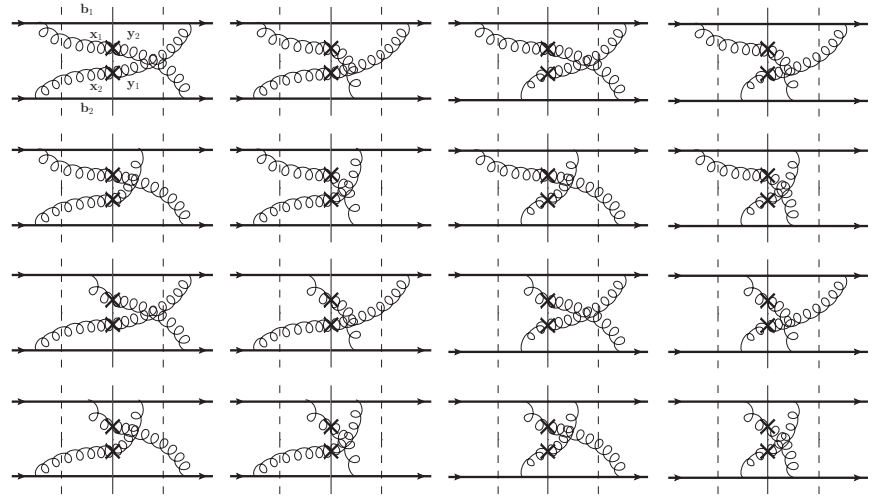
near-side correlations

$$\sim \frac{1}{(\mathbf{k}_1 - \mathbf{k}_2)^2}$$

(cf. Dumitru, Gelis, McLerran, Venugopalan '08)

Two-gluon production: properties

- Crossed diagrams at lowest nontrivial order



$$\sim \cos 2\Delta\phi \left[\frac{1}{(\mathbf{k}_1 - \mathbf{k}_2)^2} + \frac{1}{(\mathbf{k}_1 + \mathbf{k}_2)^2} \right]$$

Stronger correlations!

Two-gluon production: properties

$$\begin{aligned}
 \frac{d\sigma}{d^2k_1 dy_1 d^2k_2 dy_2} &= \frac{\alpha_s^2 C_F^2}{16 \pi^8} \int d^2B d^2b_1 d^2b_2 T_1(\mathbf{B} - \mathbf{b}_1) T_1(\mathbf{B} - \mathbf{b}_2) d^2x_1 d^2y_1 d^2x_2 d^2y_2 e^{-i \mathbf{k}_1 \cdot (\mathbf{x}_1 - \mathbf{y}_1) - i \mathbf{k}_2 \cdot (\mathbf{x}_2 - \mathbf{y}_2)} \\
 &\times \frac{\mathbf{x}_1 - \mathbf{b}_1}{|\mathbf{x}_1 - \mathbf{b}_1|^2} \cdot \frac{\mathbf{y}_1 - \mathbf{b}_1}{|\mathbf{y}_1 - \mathbf{b}_1|^2} \frac{\mathbf{x}_2 - \mathbf{b}_2}{|\mathbf{x}_2 - \mathbf{b}_2|^2} \cdot \frac{\mathbf{y}_2 - \mathbf{b}_2}{|\mathbf{y}_2 - \mathbf{b}_2|^2} \\
 &\times \left\langle \left(\frac{1}{N_c^2 - 1} \text{Tr}[U_{\mathbf{x}_1} U_{\mathbf{y}_1}^\dagger] - \frac{1}{N_c^2 - 1} \text{Tr}[U_{\mathbf{x}_1} U_{\mathbf{b}_1}^\dagger] - \frac{1}{N_c^2 - 1} \text{Tr}[U_{\mathbf{b}_1} U_{\mathbf{y}_1}^\dagger] + 1 \right) \right. \\
 &\times \left. \left(\frac{1}{N_c^2 - 1} \text{Tr}[U_{\mathbf{x}_2} U_{\mathbf{y}_2}^\dagger] - \frac{1}{N_c^2 - 1} \text{Tr}[U_{\mathbf{x}_2} U_{\mathbf{b}_2}^\dagger] - \frac{1}{N_c^2 - 1} \text{Tr}[U_{\mathbf{b}_2} U_{\mathbf{y}_2}^\dagger] + 1 \right) \right\rangle
 \end{aligned}$$

- The cross section is symmetric under (ditto for the “crossed” term)

$$\mathbf{k}_1 \leftrightarrow \mathbf{k}_2 \quad (\text{just coordinate relabeling})$$

$$\mathbf{k}_2 \rightarrow -\mathbf{k}_2 \quad \text{as} \quad \text{Tr} [U_{\mathbf{x}} U_{\mathbf{y}}^\dagger] = \text{Tr} [U_{\mathbf{y}} U_{\mathbf{x}}^\dagger]$$

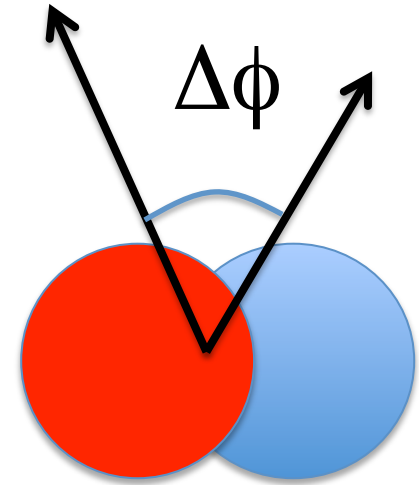
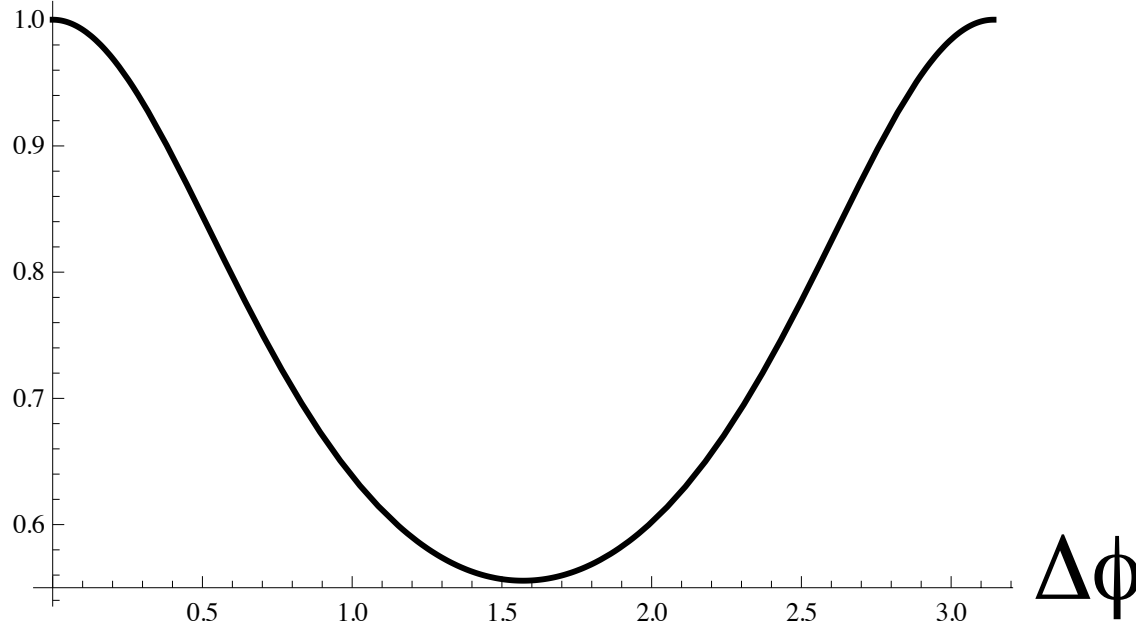
- Hence the correlations generate only even azimuthal harmonics

$$\sim \cos 2n (\phi_1 - \phi_2)$$

Correlation function

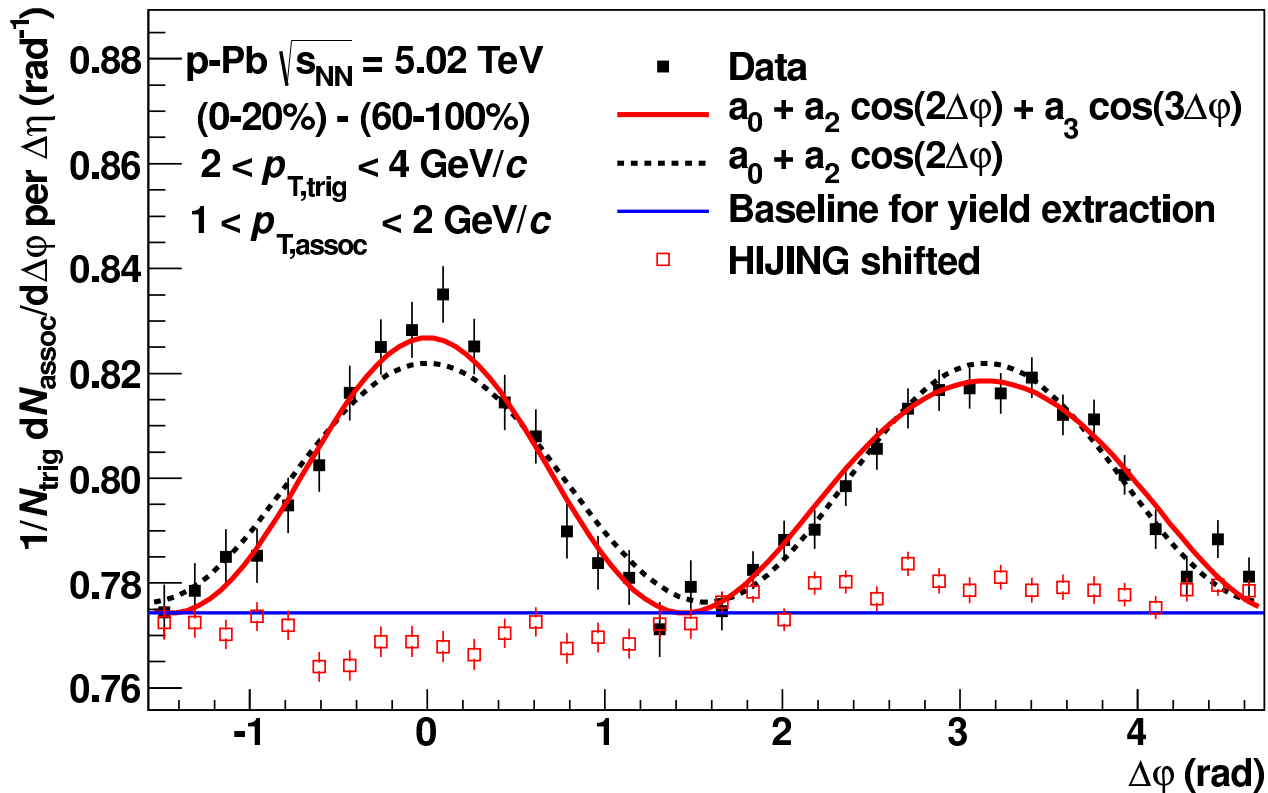
May look like this (a toy model; two particles far separated in rapidity, jets subtracted, pA and AA):

$$C(\Delta\phi)$$



Dumitru, Gelis, McLerran, Venugopalan '08; Kovner, Lublinsky '10;
Yu.K., D. Wertepny '12; Lappi, Srednyak, and Venugopalan '09

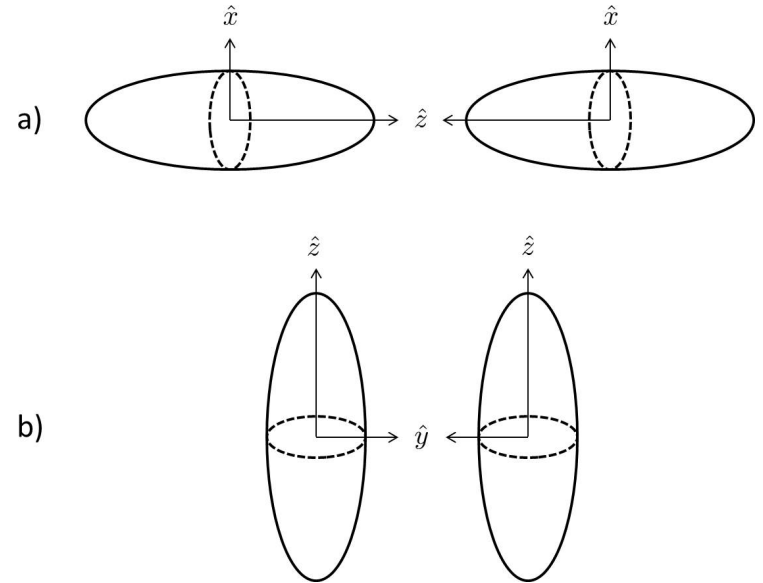
LHC p+Pb data from ALICE



- These are high-multiplicity collisions: it is possible that quark-gluon plasma is created in those collisions, with the hydrodynamics contributing to these correlations.
- Saturation approach is lacking the odd harmonics, like $\cos(3\Delta\phi)$, etc. Can they be generated by corrections to the leading-order CGC calculation?

Initial vs final-state correlations: U+U

- Hydro conventional wisdom: eccentricity is higher in side-by-side collisions, and the flow harmonics are larger.
- Saturation approach: local saturation scale is larger in tip-on-tip collisions, making correlations stronger as well.



$$\frac{C_{tip-on-tip}(\mathbf{k}_1, y_1, \mathbf{k}_2, y_2)|_{LO}}{C_{side-on-side}(\mathbf{k}_1, y_1, \mathbf{k}_2, y_2)|_{LO}} = \frac{1}{\lambda} \approx 1.26 \quad (\text{for } U + U)$$

Qualitatively different behavior in the two approaches!

$$\rho(\vec{\mathbf{r}}) = \rho_0 e^{-\frac{x^2}{R^2} - \frac{y^2}{R^2} - \frac{\lambda^2}{R^2} z^2}$$

Energy (ln)dependence

- “Glasma graphs” correlation function has the same number of Q_s factors in the numerator and the denominator:

$$C(\mathbf{k}_1, y_1, \mathbf{k}_2, y_2)|_{LO} \propto \frac{\int d^2 B d^2 b [T_1(\mathbf{B} - \mathbf{b})]^2 Q_{s2}^4(\mathbf{b})}{\int d^2 B d^2 b_1 d^2 b_2 T_1(\mathbf{B} - \mathbf{b}_1) T_1(\mathbf{B} - \mathbf{b}_2) Q_{s2}^2(\mathbf{b}_1) Q_{s2}^2(\mathbf{b}_2)}$$

- Loosely-speaking, since each saturation scale is proportional to a power of energy,

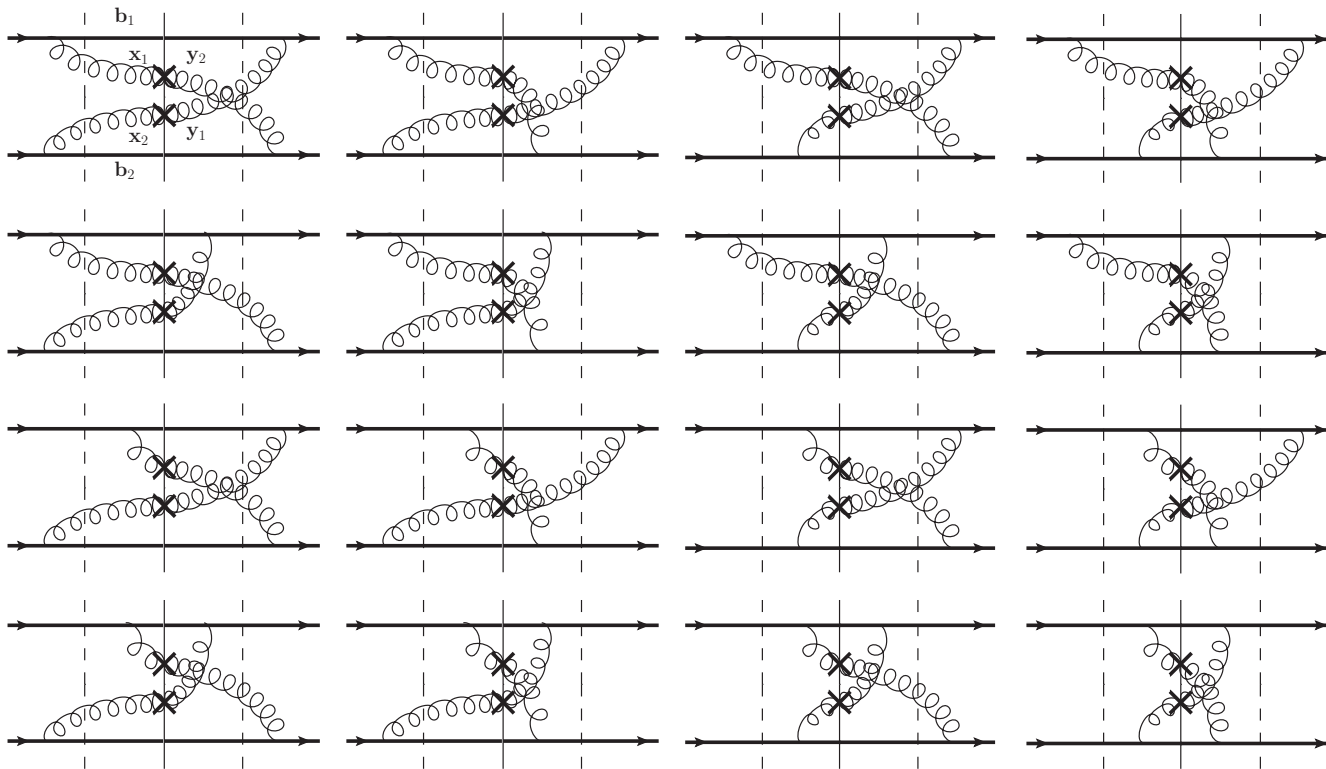
$$Q_s^2 \sim s^\lambda$$

the energy dependence cancels, and the correlation function is (almost) **energy-independent!**

C. HBT correlations

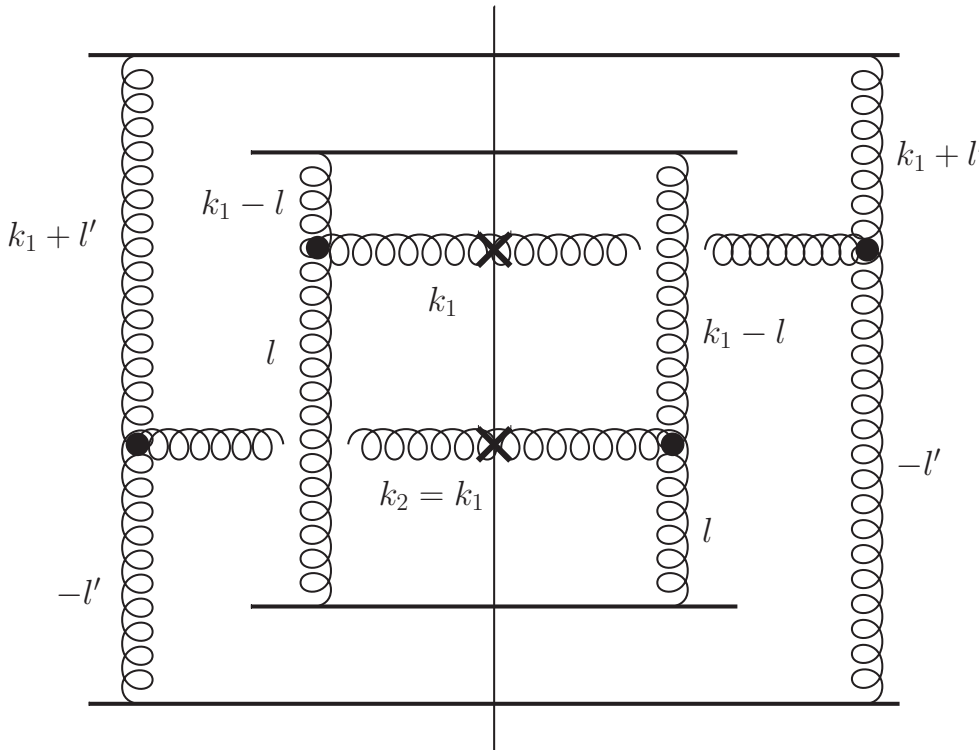
HBT diagrams

- There is another contribution coming from the “crossed” diagrams



HBT diagrams

- They give HBT correlations (with $R_{\text{long}} = 0$ due to Lorentz contraction)



$$\sim \delta^2(\mathbf{k}_1 - \mathbf{k}_2)$$

- Just like the standard HBT correlations

$$|\Psi_1(\mathbf{k}_1) \Psi_2(\mathbf{k}_2) + \Psi_1(\mathbf{k}_2) \Psi_2(\mathbf{k}_1)|^2 \rightarrow \Psi_1(\mathbf{k}_1) \Psi_2(\mathbf{k}_2) \Psi_1^*(\mathbf{k}_2) \Psi_2^*(\mathbf{k}_1) + c.c. + \dots$$

- Possibly fragmentation would break phase coherence making these perturbative HBT correlations not observable.

Back-to-back HBT?

- Note that all our formulas are symmetric under

$$\mathbf{k}_2 \rightarrow -\mathbf{k}_2$$

- Therefore, the HBT correlation is accompanied by the identical back-to-back HBT correlation

$$\sim \delta^2(\mathbf{k}_1 + \mathbf{k}_2)$$

- Note again that this correlation may be destroyed in hadronization.

k_T -Factorization?

In search of factorization

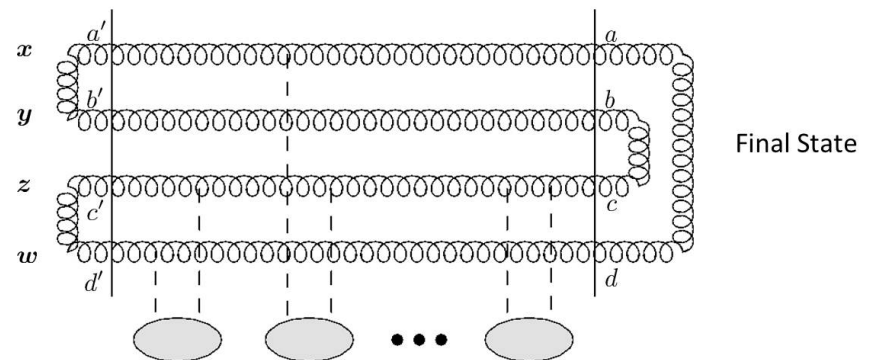
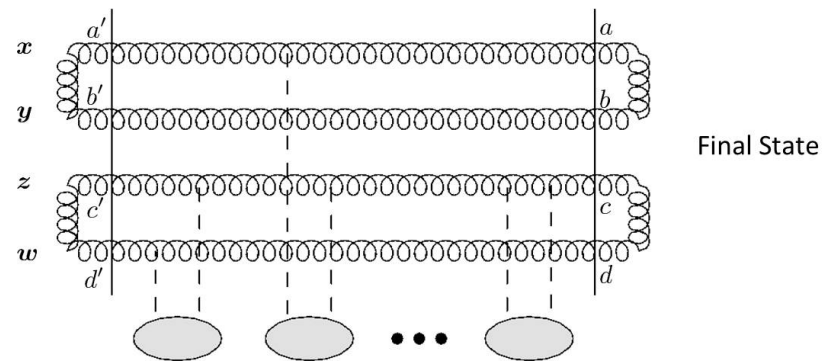
- Since a lot of CGC ‘ridge’ phenomenology was done using a k_T -factorized expression, it is natural to try to see whether our two-gluon production cross section can be written in a factorized form.
- The answer is ‘yes’, but factorization does not come naturally.

Two-gluon Distribution Functions

- Unintegrated single-gluon distribution (gluon TMD) can be defined through a (gluon) dipole operator N_G .

$$\left\langle \frac{d\phi_{A_1}(\mathbf{q}, y)}{d^2b} \right\rangle_{A_1} = \frac{C_F}{\alpha_s(2\pi)^3} \int d^2r e^{-i\mathbf{q}\cdot\mathbf{r}} \nabla_{\mathbf{r}}^2 N_G(\mathbf{b} + \mathbf{r}, \mathbf{b}, y)$$

- The two-gluon distributions can be defined either through a double-trace or the quadrupole operators:



Two-gluon Distribution Functions

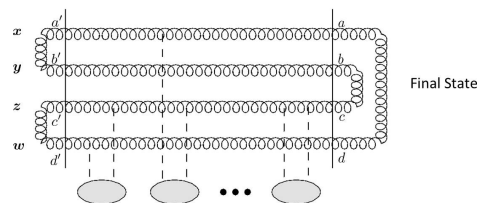
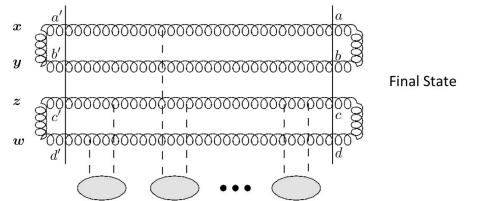
- The two-gluon distributions are:

$$\left\langle \frac{d\phi_{A_2}^{D,Q}(\mathbf{q}_1, \mathbf{q}_2, y)}{d^2b_1 d^2b_2} \right\rangle_{A_2} = \left(\frac{C_F}{\alpha_s (2\pi)^3} \right)^2 \int d^2r_1 d^2r_2 e^{-i\mathbf{q}_1 \cdot \mathbf{r}_1 - i\mathbf{q}_2 \cdot \mathbf{r}_2} \nabla_{\mathbf{r}_1}^2 \nabla_{\mathbf{r}_2}^2 N_{D,Q}(\mathbf{b}_1 + \mathbf{r}_1, \mathbf{b}_1, \mathbf{b}_2 + \mathbf{r}_2, \mathbf{b}_2, y)$$

where the double-trace and quadrupole operators are

$$N_D(\mathbf{x}, \mathbf{y}, \mathbf{z}, \mathbf{w}, Y) = \frac{1}{(N_c^2 - 1)^2} \langle \text{Tr} [1 - U_{\mathbf{x}} U_{\mathbf{y}}^\dagger] \text{Tr} [1 - U_{\mathbf{z}} U_{\mathbf{w}}^\dagger] \rangle_{A_2}(Y)$$

$$N_Q(\mathbf{x}, \mathbf{y}, \mathbf{z}, \mathbf{w}, Y) = \frac{1}{N_c^2 - 1} \langle \text{Tr} [(1 - U_{\mathbf{x}} U_{\mathbf{y}}^\dagger) (1 - U_{\mathbf{z}} U_{\mathbf{w}}^\dagger)] \rangle_{A_2}(Y)$$



k_T -Factorization

- After some algebra the two-gluon inclusive production cross section can be written in a factorized form:

$$\frac{d\sigma}{d^2k_1 dy_1 d^2k_2 dy_2} = \left(\frac{2\alpha_s}{C_F}\right)^2 \frac{1}{k_1^2 k_2^2} \int d^2B d^2b_1 d^2b_2 \int d^2q_1 d^2q_2 \left\langle \frac{d\phi_{A_1}(\mathbf{q}_1, y=0)}{d^2(\mathbf{B}-\mathbf{b}_1)} \right\rangle_{A_1} \left\langle \frac{d\phi_{A_1}(\mathbf{q}_2, y=0)}{d^2(\mathbf{B}-\mathbf{b}_2)} \right\rangle_{A_1} \\ \times \left\{ \left\langle \frac{d\phi_{A_2}^D(\mathbf{q}_1 - \mathbf{k}_1, \mathbf{q}_2 - \mathbf{k}_2, y)}{d^2b_1 d^2b_2} \right\rangle_{A_2} + \left[\frac{\mathcal{K}(\mathbf{b}_1, \mathbf{b}_2, \mathbf{k}_1, \mathbf{k}_2, \mathbf{q}_1, \mathbf{q}_2)}{N_c^2 - 1} \left\langle \frac{d\phi_{A_2}^Q(\mathbf{q}_1 - \mathbf{k}_1, \mathbf{q}_2 - \mathbf{k}_2, y)}{d^2b_1 d^2b_2} \right\rangle_{A_2} + (\mathbf{k}_2 \rightarrow -\mathbf{k}_2) \right] \right\}$$

with a somewhat involved (but known) coefficient function K .

- The expression is rather convoluted, and the function K depends on the nucleons' positions... The expression is different from what was used in phenomenology.

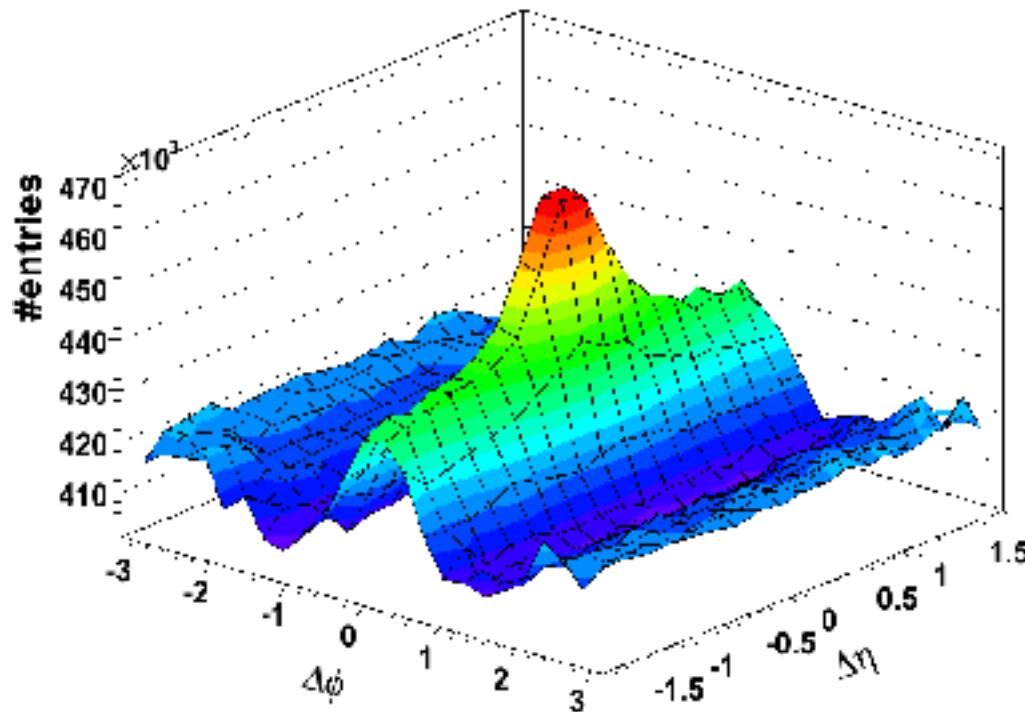
Conclusions

- We completed a calculation of the two-gluon inclusive production cross section in nuclear collisions including saturation effects in one nucleus to all orders (heavy-light ion collisions).
- Correlations we see:
 - Geometric correlations ✓
 - HBT correlations (along with b2b HBT ones)
 - Away-side correlations ✓
 - Near-side long-range rapidity correlations ✓
(✓ = long-range in rapidity)
- Near- and away-side correlations are identical to all orders in saturation effects: this is mainly consistent with the p+Pb data from LHC. Odd harmonics are missing.
- Long-range rapidity correlations are (almost) energy-independent.
- k_T -factorization can be obtained with 2 types of double-gluon distributions.
- It seems like geometric correlations are hard to remove by cumulants, since they depend on non-local geometry.

Backup Slides

Ridge in heavy ion collisions

- Heavy ion collisions, along with high-multiplicity p+p and p+A collisions, are known to have long-range rapidity correlations, known as ‘the ridge’:



This conclusion is consistent with the data

Long-Range Rapidity Correlations in Heavy-Light Ion Collisions

Yuri V. Kovchegov, Douglas E. Wertepny

(Submitted on 5 Dec 2012)

We study two-particle long-range rapidity correlations arising in the early stages of heavy ion collisions in the saturation/Color Glass Condensate framework, assuming for simplicity that one colliding nucleus is much larger than the other. We calculate the two-gluon production cross section while including all-order saturation effects in the heavy nucleus with the lowest-order rescattering in the lighter nucleus. We find four types of correlations in the two-gluon production cross section: (i) geometric correlations, (ii) HBT correlations, (iii) back-to-back correlations, and (iv) near-side azimuthal correlations which are long-range in rapidity. The geometric correlations (i) are due to the fact that nucleons are correlated by simply being confined within the same nucleus and may lead to long-range rapidity correlations for the produced particles without strong azimuthal angle dependence. Somewhat surprisingly, long-range rapidity correlations (iii) and (iv) have exactly the same amplitudes along with azimuthal and rapidity shapes: one centered around $\Delta \phi = \pi$ with the other one centered around $\Delta \phi = 0$ (here $\Delta \phi$ is the azimuthal angle between the two produced gluons).

We thus observe that the early-time CGC dynamics in nucleus-nucleus collisions generates azimuthal non-flow correlations which are qualitatively different from jet correlations by being long-range in rapidity. If strong enough, they have the potential of mimicking the elliptic (and higher-order even-harmonic) flow in the di-hadron correlators: one may need to take them into account in the experimental determination of the flow observables.

This conclusion is consistent with the data

Long-range angular correlations on the near and away side in p-Pb collisions at $\sqrt{s_{NN}} = 5.02$ TeV

ALICE Collaboration

(Submitted on 10 Dec 2012)

Angular correlations between charged trigger and associated particles are measured by the ALICE detector in p-Pb collisions at a nucleon-nucleon centre-of-mass energy of 5.02 TeV for transverse momentum ranges within $0.5 < p_{T,assoc} < p_{T,trig} < 4$ GeV/c. The correlations are measured over two units of pseudorapidity and full azimuthal angle in different intervals of event multiplicity, and expressed as associated yield per trigger particle. Two long-range ridge-like structures, one on the near side and one on the away side, are observed when the per-trigger yield obtained in low-multiplicity events is subtracted from the one in high-multiplicity events. The excess on the near-side is qualitatively similar to that recently reported by the CMS collaboration, while the excess on the away-side is reported for the first time. The two-ridge structure projected onto azimuthal angle is quantified with the second and third Fourier coefficients as well as by near-side and away-side yields and widths. The yields on the near side and on the away side are equal within the uncertainties for all studied event multiplicity and p_T bins, and the widths show no significant evolution with event multiplicity or p_T . These findings suggest that the near-side ridge is accompanied by an essentially identical away-side ridge.